Table 1. Clinical Characteristics of the Event and No-Event Groups

	All patients (n=186)	With event (n=39)	Without event (n=147)	P value
Age (years)	67±12	67±11	67±13	NS
Men (%)	121 (65)	25 (64)	96 (65)	NS
BMI	24±4.2	24±4.8	24±4.0	NS
Chest pain	42 (23)	11 (28)	31 (21)	NS
HbA1c (%)	7.2±1.8	6.6±1.2	7.3±1.9	0.027
Insulin	82 (44)	20 (51)	62 (42)	NS
Hypertension (%)	159 (85)	35 (90)	124 (84)	NS
Dyslipidemia (%)	106 (57)	21 (54)	85 (58)	NS
PAD (%)	27 (15)	9 (23)	18 (12)	0.088
Abnormal ECG (%)	145 (78)	34 (89)	111 (75)	0.041
CKD (stage)	3.1±1.3	3.7±1.3	2.9±1.3	0.0006
0–2/3–4/5	76/61/49	10/11/18	66/50/31	0.0053
Hemodialysis (%)	28 (15)	12 (31)	16 (11)	0.002
BMDS	2.8±5.1	5.3±6.1	2.1±4.5	0.0001
TLDS	1.3±3.0	2.3±3.7	1.0±2.7	0.04
MS	1.5±3.0	3.0±3.6	1.0±2.7	0.0002
EDV (ml)	82±46	97±52	78±43	0.01
ESV(ml)	40±38	51±43	37±35	0.0041
EF (%)	58±16	53±16	59±16	0.017

CKD 0, no CKD; BMI, body mass index; PAD, peripheral arterial disease; BMDS, total BMIPP (^{123}I-betamethyl-p-iodophenyl-pentadecanoic acid) defect score; TLDS, total TL (thallium) defect score; MS, mismatch score; EDV, end-diastolic volume; ESV, end-systolic volume; EF, ejection fraction.

Therefore, the present study aimed to clarify the prognostic value of BMIPP–TL dual SPECT among diabetic patients without a previous diagnosis of heart disease.

Methods

Patients

We extracted the data for 763 diabetic patients from among 2,653 consecutive patients who were entered into a BMIPP and TL dual SPECT imaging database between July 2003 and May 2009. The retrospectively enrolled patients met the following criteria at the time of imaging: age >20 years, no apparent episodes of either acute coronary syndrome or heart failure, no previous diagnosis of heart disease and follow-up for more than 2 years. We finally enrolled 186 patients in the present study. The main reasons for the imaging studies were screening tests for abnormal ECG (n=52), non-cardiac surgeries (n=42), multiple risk factors (n=32), chest pain (n=31) and abnormal wall motion detected by echocardiography (n=29). We assessed clinical characteristics including age, sex, coronary risk factors, body mass index, renal function, blood biochemical data, use of insulin, history of peripheral arterial disease and ECG findings. Renal function was evaluated by estimated glomerular filtration rate (in units of ml·min^{-1}·1.73m^{-2}),[11] which was categorized as ≥90 (CKD stage 1), 60–89 (stage 2), 30–59 (stage 3), 15–29 (stage 4), or <15 and dialysis (stage 5). No CKD patient was categorized as stage 0 for statistical analysis in this study. The Ethics Committee at Tokyo Women's Medical University approved the study protocol.

BMIPP and TL Dual SPECT

Patients were simultaneously injected with TL (74MBq) and BMIPP (111MBq) while resting. The BMIPP and TL dual SPECT data were acquired starting 20min thereafter using a

dual-headed gamma camera (ECAM Toshiba, Japan) equipped with low-energy general-purpose collimators. The data were acquired over 180° in 32 steps of 50s each in a 64×64 matrix with ECG gating by 8 frames per cardiac cycle. To separate the distribution of the isotopes, ^{201}TL and ^{123}I data were obtained using symmetrical 72±10 and 159±10keV windows, respectively. Images were processed using a Butterworth filter (order 8, cutoff value 0.33 cycles/pixel), and reconstructed by filtered back projection. Ejection fractions (EF), as well as end-diastolic and end-systolic volumes (EDV and ESV, respectively), were generated from TL-gated data using QGS software.

Tracer accumulation was scored in each of 17 segments of the left ventricular myocardium by 2 experienced nuclear medicine staff using a 5-point grading system (0, normal; 1, mildly reduced; 2, moderately reduced; 3, severely reduced; 4, absent) according to the American Heart Association criteria.[12] If the inferoposterior defect was larger or more severe in the TL than in the BMIPP image, the defect was considered to be caused by attenuation, and the TL defect was scored as the same as the BMIPP defect. The values were summed to obtain total defect scores (DS) for each tracer (BMDS, TLDS). A mismatch score (MS) was defined as BMDS minus TLDS.

Assessment of Clinical Outcome

The patients were followed for more than 2 years after the imaging study. The primary endpoint was defined as the first event of all-cause cardiac events including cardiac death, acute MI (AMI), severe heart failure requiring hospitalization, fatal arrhythmia and inevitable late coronary intervention because of unstable angina or the new onset of effort angina more than 3 months after the images were acquired. Deaths from unknown causes but after having an apparently severe cardiac status such as low cardiac function, severe multiple coronary stenosis or fatal arrhythmic episodes during follow-up, were regarded as
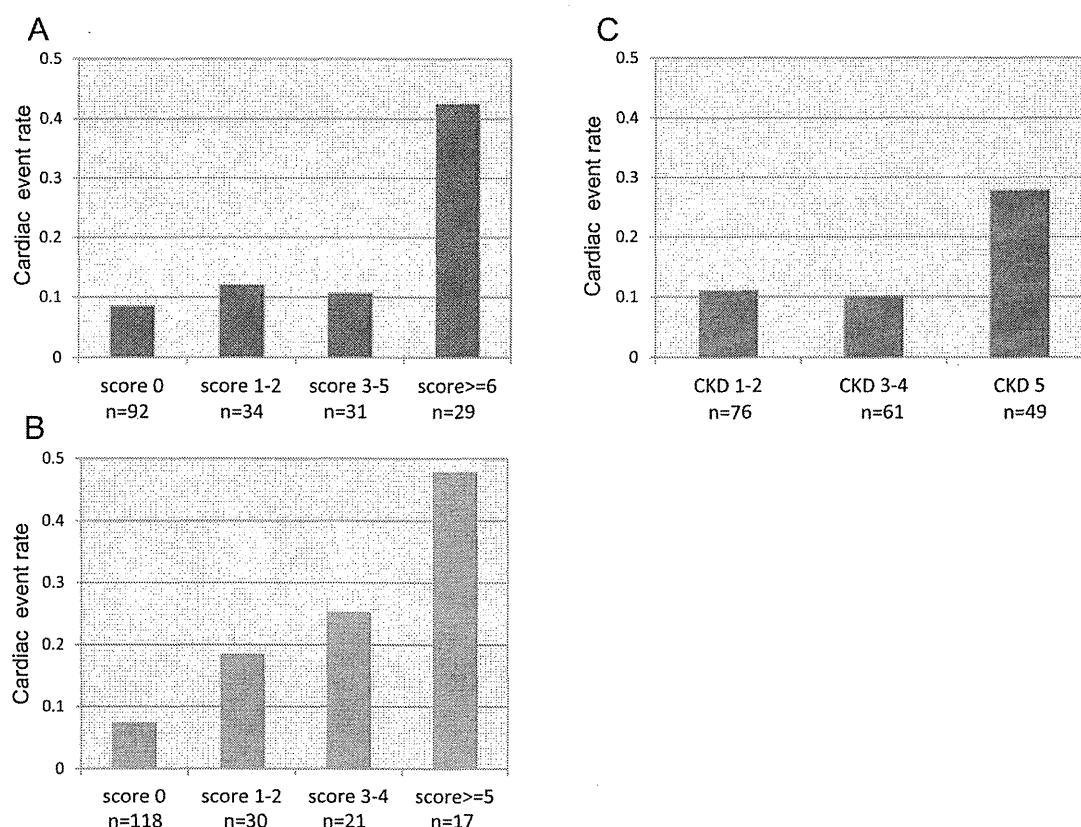
Figure 1. The 3-year cardiac event rates predicted using BMDS (A), MS (B) and CKD stage (C). The event rates are remarkably higher for BMDS ≥6, MS ≥5 and CKD stage 5 compared with other groups. BMDS, total defect score for ^{123}I-betamethyl-p-iodo-phenyl-pentadecanoic acid (BMIPP); CKD, chronic kidney disease; MS, mismatch score.

being of cardiac cause (ie, unknown cause of sudden cardiac death). The secondary endpoint was cardiac death. Patients with other unknown causes of death were censored at the endpoint for the primary and secondary outcomes. The event data were gathered from patients' records, including in-hospital or out-of-hospital reports.

Statistical Analysis

Data are expressed as average±SD of continuous variables. Continuous variables from patients with and without events were compared using the unpaired Student's t-test or the Mann-Whitney U test as appropriate, and categorical data were analyzed using the chi-square test. The independent variables in the univariate Cox proportional hazards model included age, sex, CKD stage 1–5 as a continuous variable, with/without hemodialysis (HD), presence of risk factors and imaging parameters including QGS. The relative hazard ratios and 95% confidence intervals were calculated. Moreover, among the statistically significant independent variables (P<0.05) in the univariate Cox proportional hazard model, the multivariate Cox model was applied using the forward stepwise method. Kaplan-Meier cumulative survival was analyzed using the statistically optimal threshold values of the imaging parameters. The survival curves were compared by log-rank test. Statistical significance was defined as P<0.05. Multiple comparison was used for 4-group comparisons, where the statistical sig-

nificance was defined as P<0.0083 according to the Bonferroni method.

Results

Patients' Characteristics

Table 1 shows the baseline characteristics of the patients. Frequent risk factors such as hypertension (85%), dyslipidemia (56%) and CKD (stage ≥3, 59%) in addition to DM were found in the entire group. We categorized the CKD stages as 0–2 (0 is no CKD), 3–4 and 5, because of the small study cohort and each stage comprised only a few patients (only 9 patients had stage 4 disease). The 28 patients on HD were included in CKD stage 5.

Clinical Outcomes and Prognostic Evaluation

The mean follow-up period was 3.65±1.65 years. Cardiac events were the primary outcome in 39 patients and included 8 cardiac deaths (heart failure (n=3), AMI (n=3) and unknown cause of sudden cardiac death (n=2). The nonfatal events included AMI (n=4), late revascularization because of unstable angina (n=9) and new onset of stable angina (n=9), heart failure requiring hospitalization (n=9) and fatal arrhythmia such as ventricular fibrillation or tachycardia (n=1). There were 15 noncardiac causes of death: stroke (n=1), malignancy (n=5), infectious disease (n=2), liver cirrhosis (n=1) and unknown

Table 2. Cox Hazard Univariate and Multivariate Regression Analyses

	Univariate analysis		Multivariate analysis			
	HR (CI)	P value	HR (CI) without MS	P value	HR (CI) without BMDS	P value
A. All patients (n=186)						
HbA1c	0.763 (0.605–0.962)	0.022				
Abnormal ECG	2.804 (0.996–7.897)	0.051				
CKD (stage)	1.549 (1.216–1.971)	0.0004	1.545 (1.205–1.981)	0.0006	1.568 (1.218–2.018)	0.0005
Hemodialysis	2.936 (1.484–5.809)	0.0020				
BMDS	1.076 (1.076–1.119)	0.0002	1.076 (1.033–1.120)	0.0004		
TLDS	1.087 (1.014–1.164)	0.018				
MS	1.114 (1.053–1.178)	0.0002			1.111 (1.050–1.175)	0.0003
EDV (ml)	1.006 (1.001–1.011)	0.026				
ESV(ml)	1.007 (1.001–1.013)	0.029				
EF (%)	0.977 (0.959–0.995)	0.013				
B. Patients without hemodialysis (n=158)						
HbA1c	0.799 (0.611–1.047)	0.103				
Abnormal ECG	2.636 (0.793–8.757)	0.114				
CKD (stage)	1.453 (1.065–1.982)	0.0185	1.444 (1.042–2.002)	0.0273	1.407 (1.012–1.956)	0.0424
BMDS	1.084 (1.039–1.131)	0.0002	1.082 (1.037–1.130)	0.0003		
TLDS	1.110 (1.023–1.264)	0.012				
MS	1.123 (1.057–1.194)	0.0002			1.112 (1.046–1.182)	0.0007
EDV (ml)	1.007 (1.001–1.013)	0.026				
ESV (ml)	1.008 (1.001–1.015)	0.039				
EF (%)	0.975 (0.954–0.996)	0.019				

CI, confidence interval; CKD, chronic kidney disease; HR, hazard ratio. Other abbreviations as in Table 1.
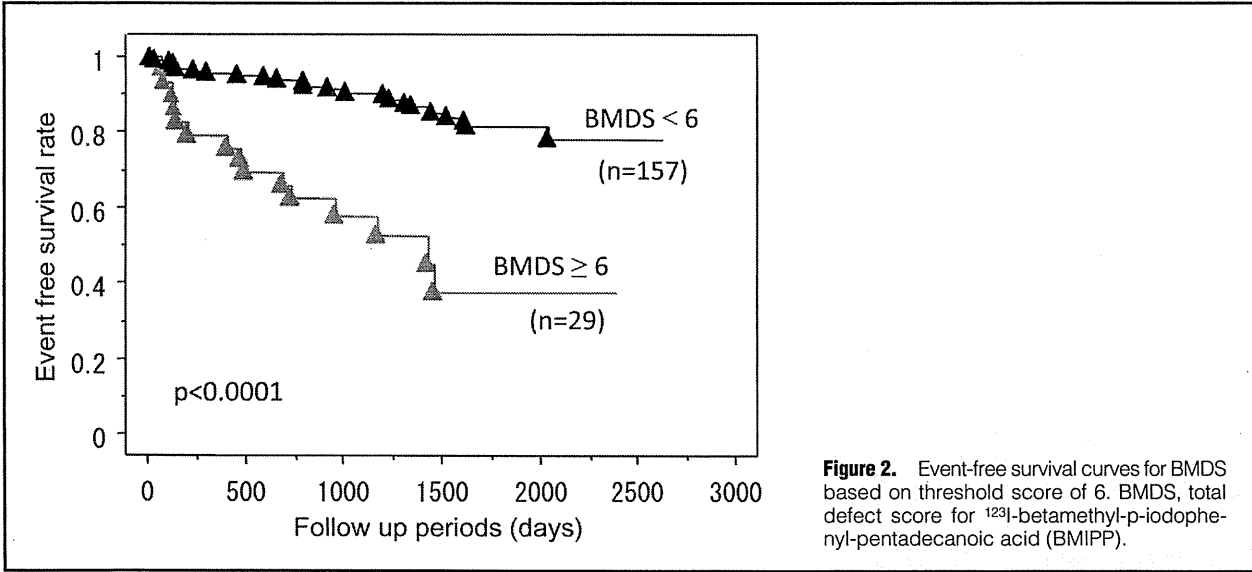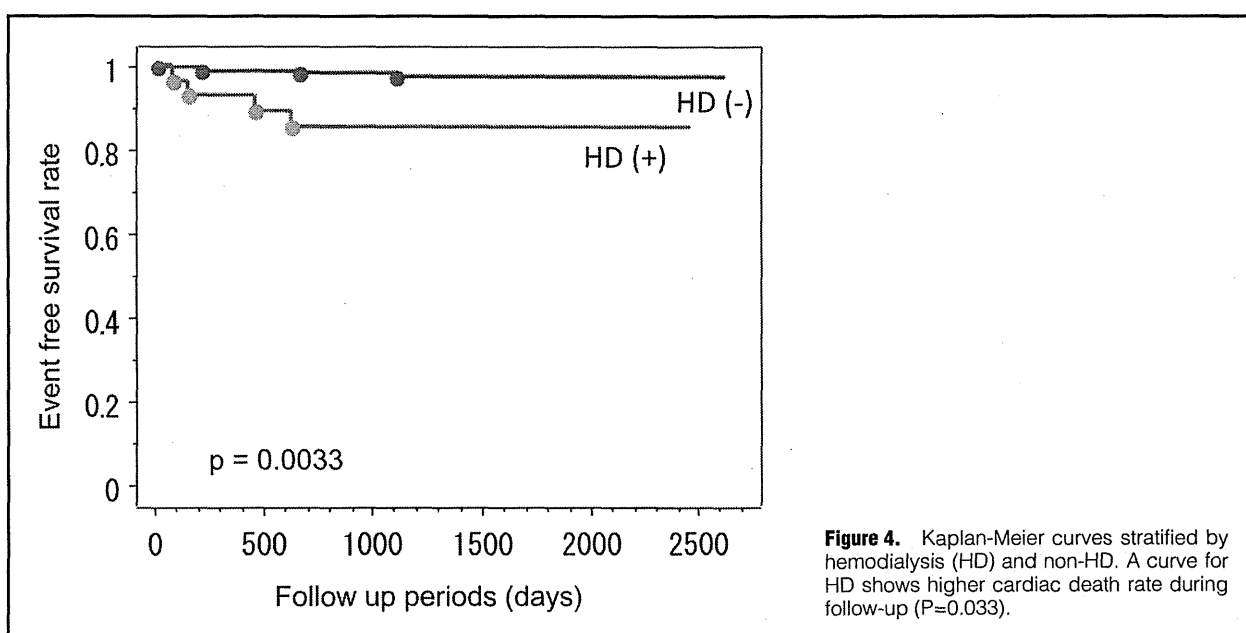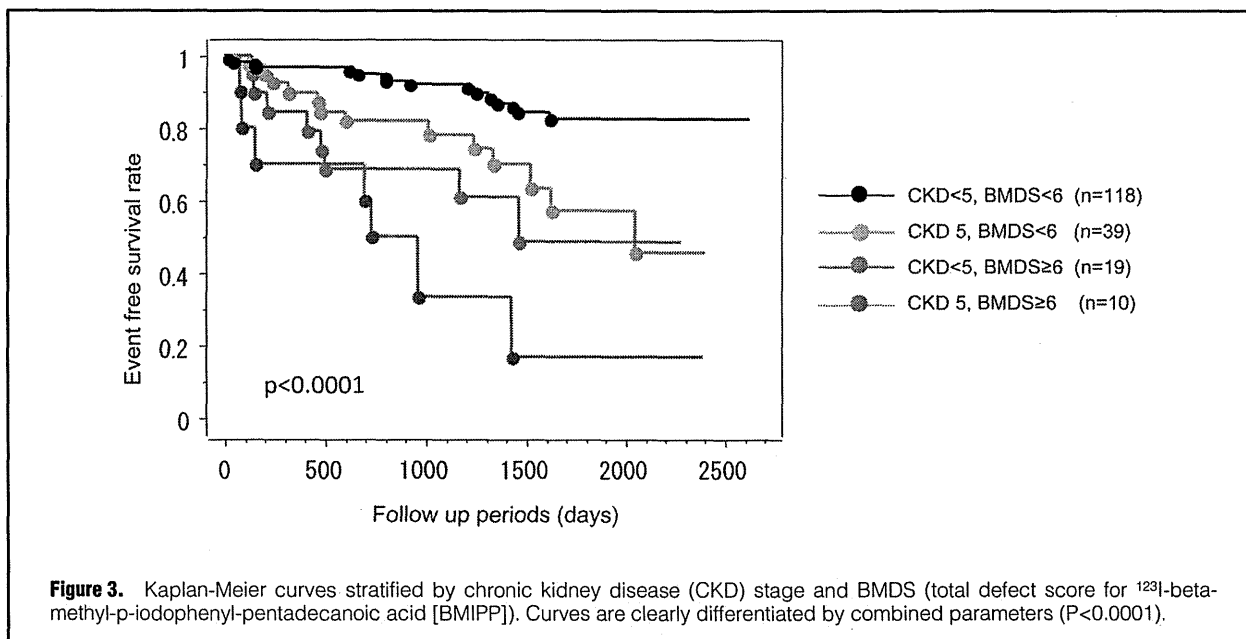

Figure 2. Event-free survival curves for BMDS based on threshold score of 6. BMDS, total defect score for ^{123}I-betamethyl-p-iodophenyl-pentadecanoic acid (BMIPP).

cause of sudden death (n=6).

Of the 3 patients who underwent revascularization within 3 months of image acquisition, 1 each developed heart failure, non-cardiac death and AMI during the follow-up.

The CKD stage was significantly higher in patients with than without all-cause cardiac events (P=0.0006), but other clinical risk factors were not significantly associated with events. HbA1c was somewhat lower in patients with events (P=0.027). More patients in the event group had an abnormal ECG (P=0.041). The imaging and functional parameters of BMDS,

TLDS, MS, EDV and ESV were significantly higher in the event group, with a significantly lower EF. Both BMDS and MS were significantly higher in patients with than without events (P=0.0001 and 0.0002, respectively).

Figure 1 shows the 3-year cardiac event rates determined using BMDS, MS and CKD stage. The event rate was considerably higher for CKD stage 5 than for lower CKD stages. Optimal cutoff values for BMDS and MS were 6 and 5, respectively as determined by receiver-operating curve analysis. Event rates for BMDS ≥6 and MS ≥5 were higher compared

Figure 3. Kaplan-Meier curves stratified by chronic kidney disease (CKD) stage and BMDS (total defect score for ^{123}I-beta-methyl-p-iodophenyl-pentadecanoic acid [BMIPP]). Curves are clearly differentiated by combined parameters (P<0.0001).

Figure 4. Kaplan-Meier curves stratified by hemodialysis (HD) and non-HD. A curve for HD shows higher cardiac death rate during follow-up (P=0.033).

with the groups with lower scores.

The prognostic value of the dual SPECT and clinical parameters selected based on the results shown in **Table 1** obtained using the Cox hazard univariate regression model for primary endpoint is shown in **Table 2**. All factors except for abnormal ECG (**Table 2A**) were significant prognostic parameters. According to the number of events (n=39), the prognostically important clinical and functional parameters of age, sex, HbA1c, HD, and CKD stage were added with the dual imaging indices and EF to the multivariate analysis. BMDS closely correlated with MS (r=0.867, P<0.0001). Among those variables, including either BMDS or MS, Cox hazard multivariate regression analysis revealed that BMDS and CKD stage (X^2=23.2, P<0.0001) or MS and CKD stage (X^2=24.3, P<0.0001) were

independent prognostic factors for cardiac events (**Table 2**). Event-free survival rates for BMDS ≥6 were much lower than those for BMDS <6 (P<0.0001) (**Figure 2**). **Figure 3** shows the Kaplan-Meier curves stratified by a combination of BMDS and CKD stage as: Group A, BMDS <6 with CKD <5 (n=118); Group B, BMDS <6 with CKD 5 (n=39); Group C, BMDS ≥6 with CKD <5 (n=19); Group D, BMDS ≥6 with CKD 5 (n=10). All patients were clearly stratified by the combination of BMDS and CKD stage (X^2=40.3, P<0.0001). Among the 4 groups, there was a significant difference in survival rate between 2 combinations as follows: Group A vs. B (P=0.0016), Group A vs. C (P=0.0003), Group A vs. D (P<0.0001).

Only HD was a significant prognostic indicator of cardiac death as the secondary endpoint (P=0.010) according to Cox

hazard univariate analysis. **Figure 4** shows the Kaplan-Meier estimates in which the curves for HD reveal a significantly higher cardiac death rate over the follow-up period (P=0.0033). Neither BMDS nor MS was a prognostic indicator for cardiac death.

In total, 12 of 28 patients on HD (43%) had cardiac events. Hemodialysis is an extremely high-risk factor for cardiac events, so we reanalyzed the patient database excluding these 28 patients. Multivariate analysis of the other 158 patients revealed that BMDS or MS and CKD class were also independent predictors for all-cause cardiac events (**Table 2B**). Among the patients, neither BMDS nor MS or other clinical risk factors including CKD class was associated with cardiac death.

Discussion

The present study found that BMIPP SPECT is of incremental value to CKD staging for stratifying prognosis among diabetic patients. A perfusion metabolic mismatch determined by BMIPP and TL SPECT reflects regions of ischemic memory of previous or continuous episodes of severe ischemia. Patients with unstable angina or AMI with early recanalization usually have a perfusion metabolic mismatch because BMIPP uptake is more easily depressed than that of TL.[9,13] Therefore, BMIPP images are a more sensitive record of myocardial ischemia than resting perfusion images.[14]

Diabetic patients are often unaware of even severe myocardial ischemia. Among the patients enrolled in the present study, although 23% of them had chest pain before the imaging study, the outcome was not associated with this symptom. In addition, BMDS, TLDS and MS did not significantly differ between patients with or without chest pain (data not shown). A chest pain episode cannot reliably indicate the severity of ischemic heart disease or of heart failure among patients with DM, so a reliable predictive clinical risk factor or examination is required to classify the likelihood of future cardiac events. The DIAD study revealed that stress myocardial perfusion imaging (MPI) did not affect the cardiac outcome among asymptomatic diabetic patients without clinically high-risk factors such as severe CKD, abnormal ECG or previous history of MI.[15] On the other hand, stress MPI has played an important role in non-invasively detecting myocardial ischemia and in predicting future events among diabetic patients with known or suspected coronary artery disease.[16] Our study population did not include cases of known coronary artery disease, but there were many patients with relatively higher risk factors such as abnormal ECG, peripheral artery disease or HD, so stress MPI may be a suitable diagnostic strategy for these patients. However, stress imaging generally requires a cardiologist for the stress test and 2 separate scans, whereas BMIPP imaging does not require a stress test and only a single injection is needed, which might render the procedure feasible enough for diabetologists to recommend it for the detection of ischemic heart disease. Our study protocol involved the simultaneous injection of both BMIPP and TL, but the results revealed that the prognostic value of MS obtained by the dual imaging was comparable to that of BMDS. Thus BMIPP single imaging is also applicable as a screening test for high-risk patients with DM.

CKD is now an established risk marker for ischemic heart disease. Cardiovascular event rates have been graded according to CKD stage.[17] A combination of CKD stage with stress imaging findings is reportedly useful for stratifying the severity of heart disease.[18,19] The present study also found that CKD was a good marker for predicting cardiac events, but the event rates increased from CKD stage 5 (**Figure 1C**), although all were low and comparable at stages 1–2 and 3–4. The different results might be because of our small study population comprising only diabetic patients. Takamura et al reported that BMDS in combination with CKD stage was useful for evaluation of cardiac events when the study population consisted of an inhomogeneous, non-HD patients who were suspected of coronary heart disease with and without previous coronary intervention.[10] The present study of only diabetic patients also discovered that BMDS in combination with CKD stage was associated with future cardiac events. Kaplan-Meier analysis using the cutoff points of BMDS 6 and CKD stage 5 could easily predict the prognosis of diabetic patients (**Figure 3**). According to the categorized data, prognostic values in patients with CKD stage 5 and BMDS <6, and in those with CKD stage <5 and BMDS ≥6, indicated relatively high and comparable event rates. Diabetic patients with stage 5 CKD might be at particularly high risk for cardiac events, and they should be carefully followed up even if the BMDS is low.

HbA1c was rather lower in patients with events because CKD stage 5 involved a lower HbA1c as is generally known.

Our previous findings suggested that diabetic patients with CKD stage 5 at the start of HD had quite a low event rate if stress SPECT confirmed the absence of myocardial ischemia.[4] BMIPP can detect severe myocardial ischemia, but it has low sensitivity for detecting stable, silent ischemia.[14] Therefore, a stress imaging study of patients with CKD stage 5 and cardiac events but low BMDS in the present study might have found silent myocardial ischemia.

BMIPP imaging could not predict cardiac death among the diabetic patients. Only HD had prognostic value for the cardiac mortality. Nishimura et al reported that BMIPP summed defect scores (BMDS) could stratify a poor prognosis for cardiac or sudden death based on a cutoff value of 12 among patients on HD, including 33% of those with diabetic nephropathy; the cardiac death rates of patients with a lower BMDS over 5 years was quite low.[20] Another study at the same institute revealed that lower BMIPP uptake and insulin resistance may be associated with cardiac death among HD patients, even without obstructive coronary artery disease.[21] The present findings contradict these results, perhaps because the characteristics of the patients differed; that is, the prevalence of cardiac events and mortality is generally higher in patients on HD. Actually, the cardiac death rate is quite low in our study (4.3%) compared with that in the previous study (27%). Patients with renal failure have a considerable amount of coronary atherosclerotic plaque,[22] which often causes sudden acute coronary syndrome even if the corresponding lesion was not stenotic before the event. In this respect, our findings result might be reasonable because to detect myocardial ischemia or a related event with non-significant coronary stenosis is difficult using BMIPP. Regardless, diabetic patients with severe renal failure, even with a low BMDS, should be given preventive medication and carefully followed. Stress MPI might be more useful to differentiate a poor prognosis among such patients. Another reason for difficulties with predicting cardiac death by BMIPP might be because many of our patients underwent coronary intervention at the first event (18 of 39 cardiac events), and none was lost through cardiac death after the event. This might have prevented secondary cardiac events, which may be the important clinical advantage for early detection of myocardial impaired fatty acid metabolism.

One limitation of this study is that a small cohort of patients was enrolled from a single institution and not all patients were fully categorized based on CKD stage or BMIPP defect score

because of a dearth of categorized data. Because CKD stage 4 usually involves a high frequency of cardiac events, it should have been independently categorized. However, the outcome of the study might be reasonable as speculated from the numbers of studies on prognostic myocardial perfusion and BMIPP.[5,8] A multicenter trial is required to confirm the prognostic significance of our findings in the same clinical setting.

Conclusion

BMIPP SPECT when combined with CKD stage is a useful tool for predicting cardiac events among diabetic patients without a history of heart disease. Diabetic patients with CKD stage 5 have a particularly poor prognosis, regardless of BMIPP SPECT findings. Further investigation in a study with a prospective design is needed to investigate whether the imaging technique is a better prognostic tool than an alternative imaging modality such as stress myocardial scintigraphy.

References

1. Haffner SM, Lehto S, Ronnemaa T, Pyorala K, Laakso M. Mortality from coronary heart disease in subjects with type 2 diabetes and in nondiabetic subjects with and without prior myocardial infarction. *N Engl J Med* 1998; **339:** 229–234.
2. De Lorenzo A, Lima RS, Siqueira-Filho AG, Pantoja MR. Prevalence and prognostic value of perfusion defects detected by stress technetium-99 m sestamibi myocardial perfusion single-photon emission computed tomography in asymptomatic patients with diabetes mellitus and no known coronary artery disease. *Am J Cardiol* 2002; **90:** 827–832.
3. Di Carli MF, Hachamovitch R. Should we screen for occult coronary artery disease among asymptomatic patients with diabetes? *J Am Coll Cardiol* 2005; **45:** 50–53.
4. Momose M, Babazono T, Kondo C, Kobayashi H, Nakajima T, Kusakabe K. Prognostic significance of stress myocardial ECG-gated perfusion imaging in asymptomatic patients with diabetic chronic kidney disease on initiation of haemodialysis. *Eur J Nucl Med Mol Imaging* 2009; **36:** 1315–1321.
5. Yamasaki Y, Nakajima K, Kusuoka H, Izumi T, Kashiwagi A, Kawamori R, et al. Prognostic value of gated myocardial perfusion imaging for asymptomatic patients with type 2 diabetes: The J-ACCESS 2 investigation. *Diabetes Care* 2010; **33:** 2320–2326.
6. Kato M, Matsumoto N, Nakano Y, Suzuki Y, Yoda S, Sato Y, et al. Combined assessment of myocardial perfusion and function by ECG-gated myocardial perfusion single-photon emission computed tomography for the prediction of future cardiac events in patients with type 2 diabetes mellitus. *Circ J* 2011; **75:** 376–382.
7. Matsuo S, Nakajima K, Yamasaki Y, Kashiwagi A, Nishimura T. Prognostic value of normal stress myocardial perfusion imaging and ventricular function in Japanese asymptomatic patients with type 2 diabetes: A study based on the J-ACCESS-2 database. *Circ J* 2010; **74:** 1916–1921.
8. Chikamori T, Fujita H, Nanasato M, Toba M, Nishimura T. Prognostic value of I-123 15-(p-iodophenyl)-3-(R,S) methylpentadecanoic acid myocardial imaging in patients with known or suspected coronary artery disease. *J Nucl Cardiol* 2005; **12:** 172–178.
9. Kawai Y, Tsukamoto E, Nozaki Y, Morita K, Sakurai M, Tamaki N. Significance of reduced uptake of iodinated fatty acid analogue for the evaluation of patients with acute chest pain. *J Am Coll Cardiol* 2001; **38:** 1888–1894.
10. Takamura T, Takahashi N, Ishigami T, Sugano T, Ishikawa T, Uchino K, et al. Combining chronic kidney disease with 201thallium/123iodine beta methyliodophenyl pentadecanoic acid dual myocardial single-photon emission computed tomography findings is useful for the evaluation of cardiac event risk. *Nucl Med Commun* 2009; **30:** 54–61.
11. Levey AS, Bosch JP, Lewis JB, Greene T, Rogers N, Roth D. A more accurate method to estimate glomerular filtration rate from serum creatinine: A new prediction equation: Modification of Diet in Renal Disease Study Group. *Ann Intern Med* 1999; **130:** 461–470.
12. Cerqueira MD, Weissman NJ, Dilsizian V, Jacobs AK, Kaul S, Laskey WK, et al. Standardized myocardial segmentation and nomenclature for tomographic imaging of the heart: A statement for healthcare professionals from the Cardiac Imaging Committee of the Council on Clinical Cardiology of the American Heart Association. *Circulation* 2002; **105:** 539–542.
13. Ito T, Tanouchi J, Kato J, Morioka T, Nishino M, Iwai K, et al. Recovery of impaired left ventricular function in patients with acute myocardial infarction is predicted by the discordance in defect size on 123I-BMIPP and 201Tl SPET images. *Eur J Nucl Med* 1996; **23:** 917–923.
14. Kawai Y, Morita K, Nozaki Y, Ohkusa T, Sakurai M, Tamaki N. Diagnostic value of 123I-betamethyl-p-iodophenyl-pentadecanoic acid (BMIPP) single photon emission computed tomography (SPECT) in patients with chest pain: Comparison with rest-stress 99 mTc-tetrofosmin SPECT and coronary angiography. *Circ J* 2004; **68:** 547–552.
15. Young LH, Wackers FJ, Chyun DA, Davey JA, Barrett EJ, Taillefer R, et al. Cardiac outcomes after screening for asymptomatic coronary artery disease in patients with type 2 diabetes: The DIAD study: A randomized controlled trial. *JAMA* 2009; **301:** 1547–1555.
16. Kang X, Berman DS, Lewin HC, Cohen I, Friedman JD, Germano G, et al. Incremental prognostic value of myocardial perfusion single photon emission computed tomography in patients with diabetes mellitus. *Am Heart J* 1999; **138:** 1025–1032.
17. Go AS, Chertow GM, Fan D, McCulloch CE, Hsu CY. Chronic kidney disease and the risks of death, cardiovascular events, and hospitalization. *N Engl J Med* 2004; **351:** 1296–1305.
18. Hakeem A, Bhatti S, Dillie KS, Cook JR, Samad Z, Roth-Cline MD, et al. Predictive value of myocardial perfusion single-photon emission computed tomography and the impact of renal function on cardiac death. *Circulation* 2008; **118:** 2540–2549.
19. Hatta T, Nishimura S, Nishimura T. Prognostic risk stratification of myocardial ischaemia evaluated by gated myocardial perfusion SPECT in patients with chronic kidney disease. *Eur J Nucl Med Mol Imaging* 2009; **36:** 1835–1841.
20. Nishimura M, Tsukamoto K, Hasebe N, Tamaki N, Kikuchi K, Ono T. Prediction of cardiac death in hemodialysis patients by myocardial fatty acid imaging. *J Am Coll Cardiol* 2008; **51:** 139–145.
21. Nishimura M, Tsukamoto K, Tamaki N, Kikuchi K, Iwamoto N, Ono T. Risk stratification for cardiac death in hemodialysis patients without obstructive coronary artery disease. *Kidney Int* 2011; **79:** 363–371.
22. Hong YJ, Jeong MH, Choi YH, Ma EH, Ko JS, Lee MG, et al. Effect of renal function on ultrasonic coronary plaque characteristics in patients with acute myocardial infarction. *Am J Cardiol* 2010; **105:** 936–942.

Creation of human cardiac cell sheets using pluripotent stem cells

Katsuhisa Matsuura [a,b], Masanori Wada [c], Tatsuya Shimizu [a], Yuji Haraguchi [a], Fumiko Sato [a],
Kasumi Sugiyama [a], Kanako Konishi [e], Yuji Shiba [d], Hinako Ichikawa [d], Aki Tachibana [c], Uichi Ikeda [d],
Masayuki Yamato [a], Nobuhisa Hagiwara [b], Teruo Okano [c,*]

[a] Institute of Advanced Biomedical Engineering and Science, Tokyo Women's Medical University, 8-1 Kawada-cho, Shinjuku, Tokyo 162-8666, Japan
[b] Department of Cardiology, Tokyo Women's Medical University, 8-1 Kawada-cho, Shinjuku, Tokyo 162-8666, Japan
[c] ABLE Corporation, 5-9 Nishigoken-cho, Shinjuku, Tokyo 162-0812, Japan
[d] Department of Cardiovascular Medicine, Shinshu University School of Medicine, 3-1-1 Asahi, Matsumoto 390-8621, Japan
[e] Asahi Kasei Co., Ltd., 1-105 Kanda Jinbo-cho, Chiyoda, Tokyo 101-8101, Japan

ARTICLE INFO

ABSTRACT

Although we previously reported the development of cell-dense thickened cardiac tissue by repeated transplantation-based vascularization of neonatal rat cardiac cell sheets, the cell sources for human cardiac cells sheets and their functions have not been fully elucidated. In this study, we developed a bioreactor to expand and induce cardiac differentiation of human induced pluripotent stem cells (hiPSCs). Bioreactor culture for 14 days produced around 8×10^7 cells/100 ml vessel and about 80% of cells were positive for cardiac troponin T. After cardiac differentiation, cardiomyocytes were cultured on temperature-responsive culture dishes and showed spontaneous and synchronous beating, even after cell sheets were detached from culture dishes. Furthermore, extracellular action potential propagation was observed between cell sheets when two cardiac cell sheets were partially overlaid. These findings suggest that cardiac cell sheets formed by hiPSC-derived cardiomyocytes might have sufficient properties for the creation of thickened cardiac tissue.

© 2012 Elsevier Inc. All rights reserved.

1. Introduction

Regenerative medicine is thought to be a promising therapeutic strategy for the treatment of severe heart failure. We previously developed an original scaffold-free tissue engineering technology, designated as "cell sheet-based tissue engineering", using temperature-responsive culture dishes covalently bonded to the temperature-responsive polymer poly(N-isopropylacrylamide) [1]. Lowering the culture temperature promotes a rapid surface transition from hydrophobic to hydrophilic, which enables collection of a viable monolayer cell sheet with full preservation of the cell-cell contacts and extracellular matrices [2]. Many studies have shown that cell sheet-based bioengineered tissue transplantation improves the cardiac function of various types of heart failure models [3–5]. However, recent evidences have suggested that paracrine mechanisms, including angiogenesis and cardioprotection mediated by the secreted factors of transplanted cells, mainly contribute

to the improved cardiac function [3,6]. Furthermore, an adult human heart is reported to contain over a billion cardiomyocytes [7], indicating that creation of bioengineered thickened cardiac tissue in vitro, which directly contributes to contraction when transplanted, might be a prerequisite. Previously, we reported the development of cell-dense 1 mm thick cardiac tissue by repeated transplantation of triple-layered neonatal rat cardiac cell sheets [8]. Recently, we have also reported the development of cardiac cell sheets derived from mouse embryonic stem cells (ESCs) after three-dimensional suspension culture [9]. Mouse ESC-derived cardiac cell sheets have similar electrophysiological properties to those of neonatal rat cardiomyocytes, indicating that layered stem cell-derived cardiac cell sheets might show synchronous contraction. However, it remains unknown whether human pluripotent stem cell-derived cardiomyocytes are suitable for creating cell sheets in terms of their electrophysiological functions.

Many recent reports have suggested that human pluripotent stem cells, including ESCs and induced pluripotent stem cells (hiPSCs), differentiate into cardiomyocytes through embryoid body (EB) formation [10,11] and monolayer culture [12,13]. Although suspension culture of EBs is easy in terms of scale-up, advancements to overcome the limitation of EB size heterogeneity for efficient cardiac differentiation might be necessary. Conversely,

the monolayer-based method is able to consistently produce cardiomyocytes with high efficacy, but scale-up might be a significant challenge. Recent methodological progress has enabled production of >80% cardiomyocytes in both methods [14,15]. However, the differences in cardiomyocyte properties from the viewpoint of cell sheet-based tissue engineering remain elusive.

The aims of this study were to establish easy and effective methods for collecting cardiomyocytes derived from hiPSCs to create cardiac cell sheets, and to elucidate the electrophysiological functions of hiPSC-derived cardiac cell sheets.

2. Materials and methods

2.1. Antibodies

The following antibodies were used for immunocytochemistry and/or flow cytometry: anti-sarcomeric α-actinin (Sigma–Aldrich, St. Louis, MO), anti-cardiac troponin T (cTnT; Thermo Scientific, Rockford, IL), anti-CD31 (BD Bioscience, San Jose, CA) and anti-Tra-1 60 (Millipore, Billerica, MA) mouse monoclonal antibodies, anti-SM22 (Abcam, Cambridge, UK), anti-connexin 43 (Enzo Life Sciences, Farmingdale, NY) and anti-von Willebrand factor (vWF, Dako, Japan) rabbit polyclonal antibodies, and an anti-Nkx2.5 goat polyclonal antibody (Santa Cruz Biotechnology Inc., Santa Cruz, CA). Secondary antibodies were purchased from Jackson Immuno-Research Laboratories (West Grove, PA). Unless specified otherwise, reagents were purchased from Life Technologies, CA.

2.2. Human iPSC culture

Human iPSCs (253G1) were purchased from RIKEN (Tsukuba, Japan) and maintained in Primate ES Cell Medium (ReproCELL, Japan) supplemented with 5 ng/ml basic fibroblast growth factor (bFGF; ReproCELL) on mitomycin C-treated mouse embryonic fibroblasts (MEFs; ReproCELL). Cells were passaged as small clumps every 3–4 days using CTK solution (ReproCELL).

For monolayer cardiac differentiation, hiPSCs were adapted and maintained on Matrigel (growth factor reduced, 1:60 dilution) in MEF-conditioned medium (MEF-CM) supplemented with 10 ng/ml bFGF. Mitomycin-C treated MEFs were seeded at approximately 6×10^5 cells/cm^2 in DMEM (Sigma–Aldrich) supplemented with 10% FBS, 2 mM L-glutamine and 1% nonessential amino acid (NEAA) onto tissue culture dishes precoated with 0.5% gelatin. One day after seeding MEFs, the culture medium was exchanged with ESC medium (80% Knock-out DMEM, 20% Knock-out Serum Replacement, 1% NEAA, 1 mM L-glutamine, 0.1 mM β-mercaptoethanol (Sigma–Aldrich) and 5 ng/ml bFGF). MEF-CM was collected everyday for 7 days and supplemented with an additional 5 ng/ml bFGF before use.

2.3. Bioreactor system

The culture process in the bioreactor system (Fig. 1A) is shown in Fig. 1B. Following CTK solution treatment, hiPSC aggregates (approximately 2×10^7 cells) from 10 culture dishes (10 cm diameter) were resuspended in 100 ml mTeSR1 (STEMCELL Technologies Inc., Canada) containing 10 μM Y27632 (Wako, Japan) and seeded into a 250 ml stirred bioreactor (Bio Jr. 8; ABLE Co., Japan). A 2-bladed delta-like paddle was used (Fig. 1A). The bioreactor was equipped with a temperature sensor, pH electrodes, as well as inoculation-, harvest- and sample-ports. Dissolved oxygen was monitored using a Fibox3 optical sensor (PreSens, Germany). Data acquisition and process control were performed with a digital control unit and process control software for the MiniJar8 100 ml bioreactor. Aeration was performed by headspace. The agitation rate

was 40 rpm, dissolved oxygen was maintained at 40% with air, oxygen or nitrogen, pH was maintained at 7.2 by CO_2 addition, and the temperature was maintained at 37 °C for the entire process. After 1 day, cells were cultured in mTeSR1 without Y27632, and the medium was exchanged every day until day 3.

2.4. Cardiac differentiation in the bioreactor

Three days after starting cultures in the bioreactor system, EBs were cultured in StemPro34 medium containing 50 μg/ml ascorbic acid (Sigma–Aldrich), 2 mM L-glutamine and 400 μM 1-thioglycerol (Sigma–Aldrich). The following growth factors and small molecule were used at the corresponding days: days 3–4, 0.5 ng/ml BMP4 (R&D systems, Minneapolis, MN); days 4–7, 10 ng/ml BMP4, 5 ng/ml bFGF, 3 ng/ml activin A (R&D Systems); days 7–9, 4 μM IWR-1 (Wako); after day 9, 5 ng/ml VEGF (R&D Systems) and 10 ng/ml bFGF. At days 4, 7, 9, 11 and 14, the culture medium was exchanged.

2.5. Cardiac differentiation in a monolayer

Cardiac differentiation was induced as previously reported with a few modifications as shown Fig. 1C. hiPSCs cultured in MEF-CM on Matrigel were treated with versene for 7–10 min, and then the single cell suspension was seeded onto Matrigel-coated dishes at 1×10^5 cells/cm^2 in MEF-CM with an additional 5 ng/ml bFGF and 10 μM Y27632 at 3 days before cardiac induction. One day before cardiac induction, cells were covered with Matrigel (1:60 dilution). For cardiac induction, the medium was changed to RPMI 1640 containing B27 supplement without insulin. The following growth factors were used at the corresponding days; days 0–1, 100 ng/ml activin A; days 1–4, 10 ng/ml BMP4 and 10 ng/ml bFGF. After day 4, cells were cultured without any growth factors, and the culture medium was changed every other day.

2.6. Flow cytometric analysis

Cells at day 14 in the bioreactor and at day 12 in monolayer culture were dissociated with Accumax (Millipore) for 10 min. Tra-1 60 staining was performed according to the manufacturer's instructions for the antibody. For CD31 staining, the antibody was diluted in PBS containing 5% FBS. For cTnT staining, cells were fixed with 4% paraformaldehyde for 10 min, and then stained with the antibody diluted in PBS with 5% FBS and 0.2% Nonidet P 40 (Nacalai Tesque, Japan). Stained cells were analyzed using a Quanta (Beckman Coulter, Brea, CA) and Quanta SC software.

2.7. Immunocytochemistry

Cells were fixed with 4% paraformaldehyde, and the immunostaining methods have been described previously [3]. Samples were imaged by laser confocal microscopy (Carl Zeiss, Germany) and Image Express (Molecular device, Sunnyvale, CA) with MetaXpress and AcuityXpress software (Molecular device).

2.8. Cell sheet preparation

Prior to seeding cells, the surface of temperature-responsive dishes (UpCell; CellSeed, Japan) was coated with FBS for 2 h. After cardiac differentiation, cells were dissociated with 0.05% trypsin/EDTA, cell aggregates were removed using a strainer (BD Bioscience), and single cells were plated onto the UpCell at 2.1×10^5 cells/cm^2 in DMEM supplemented with 10% FBS and 10 μM Y27632 at 37 °C in a humidified atmosphere with 5% CO_2. At days 1 and 3, the medium was exchanged with prewarmed DMEM supplemented with 10% FBS. After 5 days in culture, cell sheets were
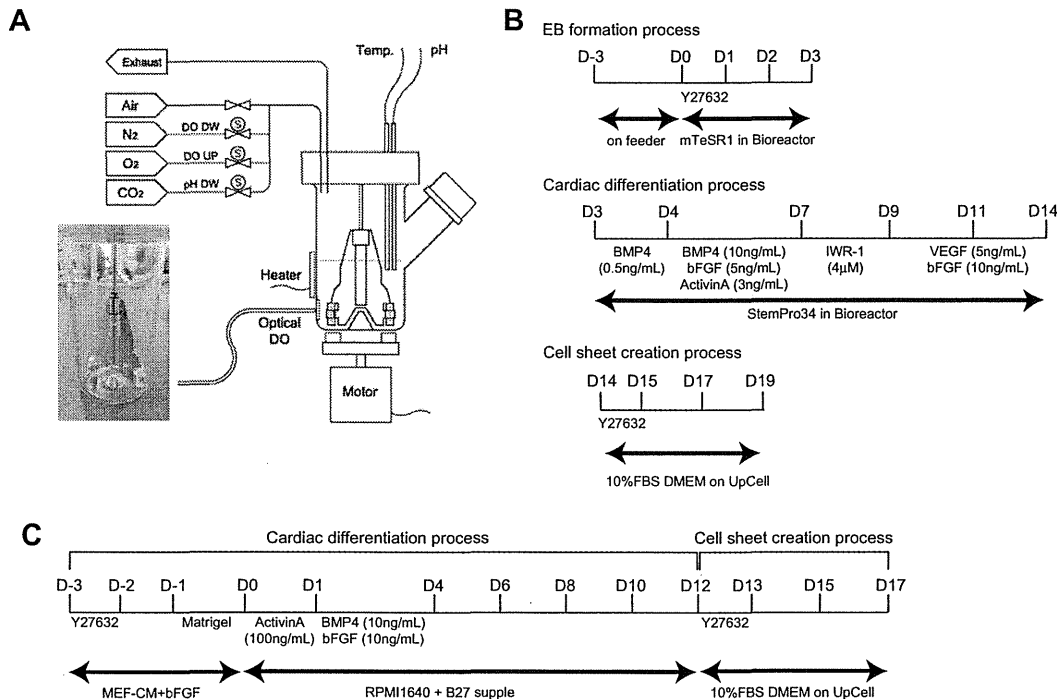
Fig. 1. Scheme of the bioreactor and culture process (A) Schematic of the bioreactor system. The photograph shows the impeller. (B) Schematic of the culture process for cardiac differentiation in the bioreactor system. (C) Schematic of the culture process for cardiac differentiation in monolayer culture.

harvested and layered using the cell sheet stacking technique as described previously[9].

2.9. Electrophysiological analysis

Electrical activities of cardiomyocyte sheets were obtained from extracellular potentials measured by a multi-electrode array (MED) system (Alpha MED Sciences, Osaka, Japan) as described previously[9]. Intracellular calcium transient of cardiomyocytes in the cell sheet was visualized using a Rhod-3 imaging kit (Life Technologies) according to the manufacturer's instructions. Fluorescence and phase contrast images were obtained by a CCD camera (HiSCA, HAMAMATSU, Japan) connected to the fluorescence microscope (ELIPSE TE2000-U, Nikon, Japan).

2.10. Statistics

Data were presented as the means ± standard deviation.

3. Results

3.1. Cardiac differentiation of hiPSCs

Various types of methods to induce cardiac differentiation of human pluripotent stem cells have been reported [10–12]. In this study, we used two types of methods; (1) suspension culture in the bioreactor, and (2) monolayer culture. Small aggregates of hiP-SCs (approximately 2×10^7 cells) were seeded in the bioreactor containing mTeSR1 medium, resulting in the formation of many EBs, and the cell number increased up to around 4×10^7 cells at day 3 (Fig. 2A and B). Then, EBs were treated with several growth factors and a Wnt inhibitor as shown in Fig. 1B. At day 14, the cell number was slightly increased to around 8×10^7 cells (Fig. 2B), and almost all of the remaining EBs showed spontaneous beating

(Supplementary Video 1). Z-stack images of immunocytochemical analysis showed that numerous areas of EBs were composed of cTnT-positive cardiomyocytes (Fig. 2C). Furthermore, almost all cTnT-positive cells expressed Nkx2.5 and SM22 (Fig. 2D), suggesting that differentiated cardiomyocytes showed a fetal phenotype. On the other hand, vWF-positive endothelial cells were distributed in minor areas (Fig. 2C), but showed a microvascular network (Fig. 2E). Flow cytometric analysis revealed that about 80% of cells were positive for cTnT, 5% of cells were positive for CD31 and 1% of cells were positive for Tra-1 60 (Fig. 2F). These findings indicate that bioreactor-based EB suspension culture with suitable growth factor and small molecule treatments might sufficiently induce cardiac differentiation of hiPSCs to create cell sheets.

Next, we induced cardiac differentiation of hiPSCs in monolayer culture (Fig. 1C). Spontaneously beating cells were observed from day 10, and robust pulsation was observed macroscopically all over the culture dish at day 12 (Video 2). Flow cytometric analysis showed that about 80% of cells were positive for cTnT (Fig. 2G). Furthermore, cardiac differentiated cells expressed cTnT and sarcomeric α-actinin with a fine striated pattern (Fig. 2H). The cell number was increased from 1×10^5 to 3.5×10^5 cells/cm^2 at day 12 (Fig. 2I). These findings suggest that the monolayer cardiac induction method might also be suitable to collect sufficient cardiomyocytes to create cardiac cell sheets.

3.2. Creation of cardiac cell sheets

Next, we created cardiac cell sheets using hiPSC-derived cardiomyocytes and UpCell temperature-responsive culture dishes. After cardiac differentiation in the bioreactor, cells were dissociated with trypsin and seeded onto the UpCell. One day after seeding (D15 in Fig. 1B), some spontaneously beating cells were observed (Video 3). Moreover the number of spontaneously beating cells increased over time, and synchronous beating over the entire dish
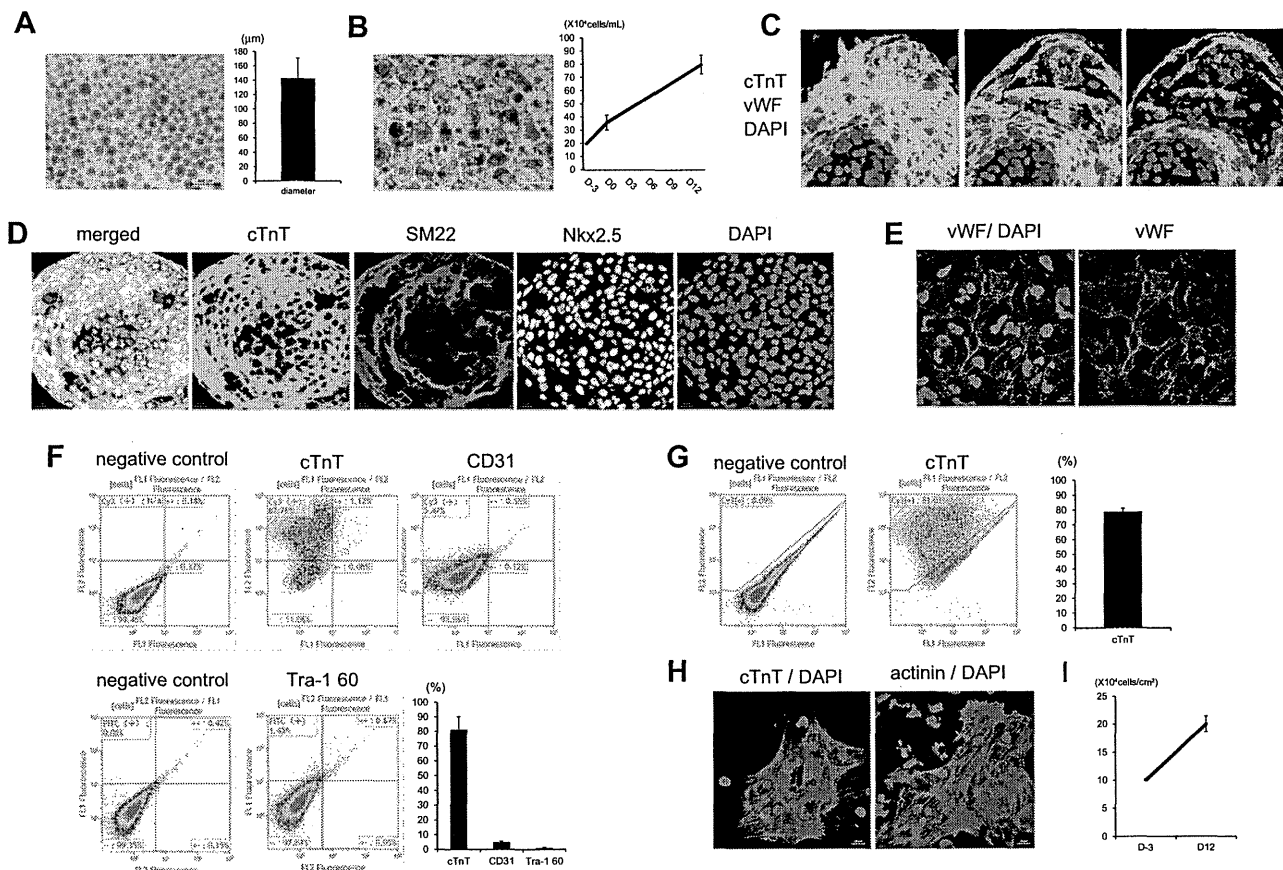
Fig. 2. Cardiac differentiation of hiPSCs (A–F) Results of the bioreactor experiments. (A) Representative image (left) and the diameter (right) of EBs at day 3. Bar, 500 μm. (B) Representative image of EBs at day 15 (left). Bar, 500 μm. Right, the cell number during bioreactor culture. (C) Z-stack images of EBs stained for cTnT (green) and vWF (red). The interval between images is 80 μm. Nuclei were stained with DAPI. Bar, 20 μm. (D) Almost all cells in EBs consisted of cTnT-positive cells that co-expressed Nkx2.5 and SM22. Nuclei were stained with DAPI. Bars, 20 μm. (E) Endothelial microvascular networks in EBs. Endothelial cells were stained for vWF. Nuclei were stained with DAPI. Bars, 20 μm. (F) Flow cytometric analyses at day 15. The percentage of cells expressing each protein was calculated and shown in the graph (n = 2). (G–I) Results of monolayer culture experiments. (G) Flow cytometric analyses at day 15. The percentage of cTnT-positive cells was calculated and shown in the graph (n = 3). (H) Differentiated cells expressed cTnT (left) and sarcomeric α-actinin (right). Nuclei were stained with DAPI. Bars, 20 μm. (I) The cell number during monolayer culture.

was observed at day 5 (D19 in Fig. 1B) (Video 4). Cells were cultured in a 20 °C incubator to create a cell sheet (Fig. 3A) that showed synchronous and spontaneous contraction when floating (Video 5). To examine the cell distribution and components in the cell sheets, immunocytochemical analysis was performed. High content confocal image analysis revealed that about 80–90% of cells were positive for cTnT and sarcomeric α-actinin and these cells also expressed Nkx2.5 and SM22 (Fig. 3C and E), indicating that the percentage of cardiomyocytes in the cell sheets was consistent with the results of flow cytometric analyses of EBs (Fig. 2F). On the other hand, almost all of the non-cardiomyocyte area was filled with SM22-positive cells without co-expression of cTnT (Fig. 3B, C and E), suggesting the presence of mural cells. We also observed a very small number of vWF-positive endothelial cells in cell sheets (Fig. 3D). These findings indicate that cardiac cell sheets were mainly composed of cardiomyocytes and mural cells.

We also created cardiac cell sheets using cardiomyocytes obtained by differentiation in monolayer culture. Cells were dissociated with trypsin and seeded onto the UpCell, which showed spontaneous and synchronous beating cells after 3 days of culture (D15 in Fig. 1C) (Video 6). However, cardiomyocytes showed colony formation (Fig. 3F and G) that led to an unequal distribution of cardiomyocytes in the cell sheets. These findings suggest that different cardiomyocyte characteristics result from bioreactor- and monolayer-based cardiac inductive methods, and cardiomyo-

cytes obtained from bioreactor-based cardiac differentiation are more suitable for creating cell sheets in the current protocol.

3.3. Electrophysiological evaluation of hiPSC-derived cardiac cell sheets

Consistent with the results of cardiomyocytes in cell sheets showing spontaneous and synchronous beating, connexin 43 expression was observed at the edge of adjacent cardiomyocytes (Fig. 4A). To confirm the electrophysiological connections among cardiomyocytes in cell sheets, extracellular action potentials were measured using the MED system. As shown in Fig. 4B, synchronous extracellular action potential excitation was observed in all areas. Furthermore, to clarify the electrophysiological connections between cell sheets, a cell sheet was seeded onto one side of the MED system. After 30 min, another cell sheet was seeded onto the other side of the MED system. Under this condition, the two cell sheets were partially overlaid and synchronous beating in the two cell sheets was observed (Fig. 4C). Furthermore, the synchronous beating of two and three overlaid cardiac cell sheets was confirmed by the results of intracellular calcium transient images (Videos 7 and 8). These findings indicate that electrical communication was established between hiPSC-derived cardiac cell sheets.
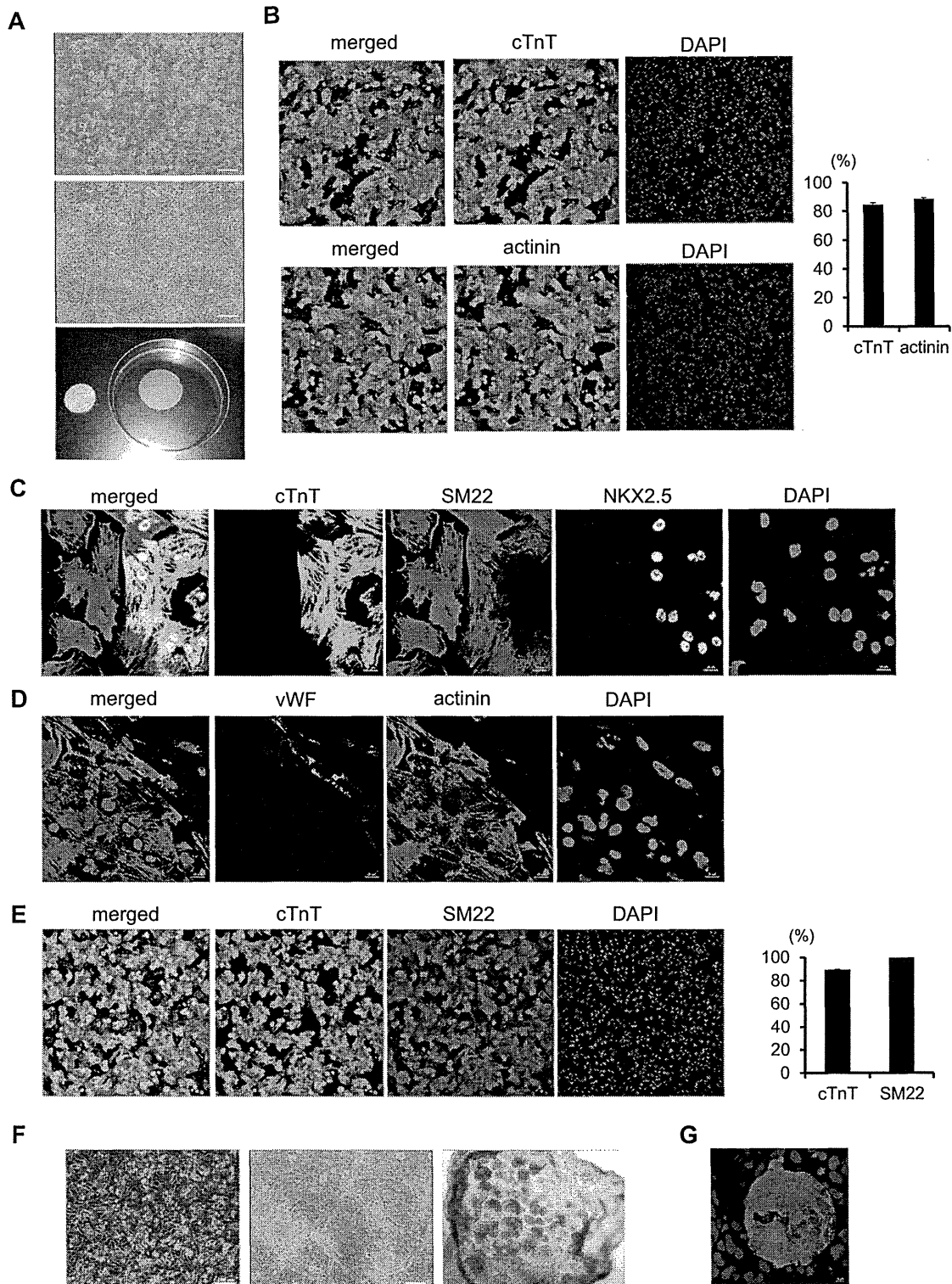
Fig. 3. Immunocytochemical evaluation of cardiac cell sheets (A–E) Results using cells from the bioreactor. (A) Representative images of cells after re-seeding on the UpCell, and a cell sheet. Upper, day 1. Middle, day 5. Bars, 100 μm. Lower, a cell sheet from a 10 cm dish. (B) Confocal image analysis of the percentage of cardiac protein-expressing cells in cell sheets. Left panels are representative images. Upper, cTnT. Lower, actinin. The percentage of cells expressing each protein was calculated and shown the graph (right). Nuclei were stained with Hoechst 33258. Original magnification, 20×. (C) The non-cardiomyocyte area was composed of SM22-positive cells that did not express cTnT or Nkx2.5. Nuclei were stained with DAPI. Bar, 20 μm. (D) Endothelial cells (vWF) in the cell sheet. Nuclei were stained with DAPI. Bar, 20 μm. (E) Confocal image analysis of the percentage of cTnT- and SM22-positive cells in cell sheets. Left panels show representative images. Nuclei were stained with Hoechst 33258. Original magnification, 20×. The percentage of cells expressing each protein was calculated and shown the graph (right). (F and G) Results using cells from monolayer culture. (F) Representative images of cells after re-seeding on the UpCell, and a cell sheet. Left, day 1. Middle, day 5. Bars, 100 μm. Right, a cell sheet from a 3.5 cm dish. Original magnification, 2×. (G) Representative confocal microscopic image of cardiomyocytes (cTnT) in a cell sheet. Nuclei were stained with DAPI. Bar, 20 μm.
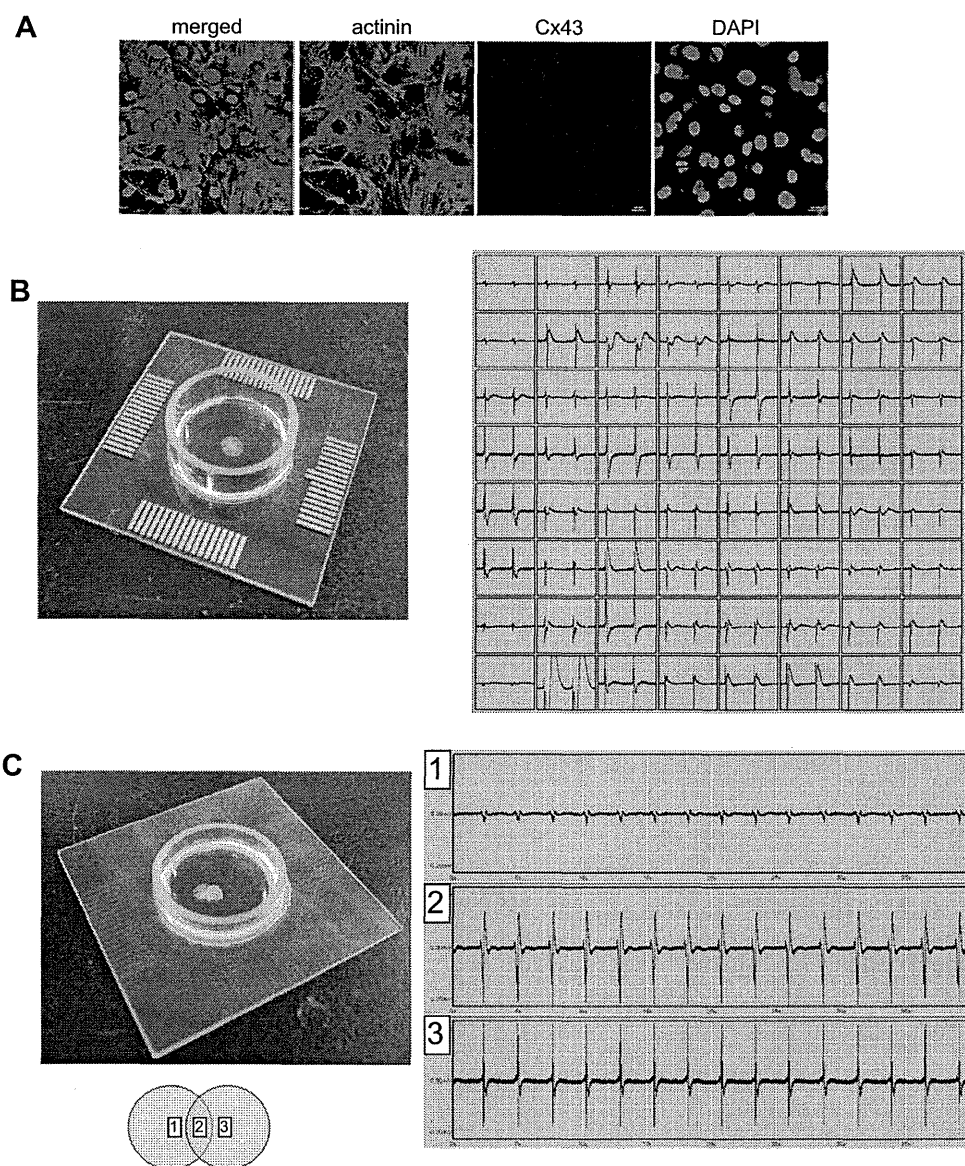
Fig. 4. Electrophysiological evaluation of cardiac cell sheets (A) Connexin 43 expression between cardiomyocytes (actinin). Nuclei were stained with DAPI. Bar, 20 μm. (B) Extracellular action potential evaluation of a monolayer cardiac cell sheet. Left panel shows a macroscopic image of the cell sheet on the MED system. Synchronous extracellular action potential excitation was observed in all areas. (C) Electrophysiological connections between cell sheets. The left panel shows a macroscopic view of partially overlaid cell sheets on the MED system. The right panel shows the extracellular action potential at each electrode position. The number in the lower panel shows the position of the electrode under the cell sheets. Number 2 is under the overlaid area.

4. Discussion

The present study shows that a bioreactor-based method sufficiently induces cardiac differentiation of around 80% of hiPSCs. Cardiomyocytes in the cell sheets showed spontaneous and synchronous beating, and the cell sheet itself showed macroscopic contraction. Furthermore, electrophysiological connections were observed between cardiac cell sheets. Therefore, human pluripotent stem cell-derived cardiac cell sheets might be used to construct functional thickened cardiac tissue.

Many reports have indicated that human pluripotent stem cells can differentiate into cardiomyocytes. EB formation is wildly used for differentiation of pluripotent stem cells, and stage-specific treatments with specific growth factors enhance cardiac differentiation [16]. Moreover, some methods, including forced aggregation, have been reported to overcome the limitation of EB size heterogeneity in terms of cardiac differentiation efficacy [14]. However, these methods are technically complex and time consuming. In this study, we have developed a suspension culture bioreactor system for cardiac differentiation. The suitable agitation system enabled formation of homogeneously sized EBs, to a certain extent, simply by seeding cell aggregates. Furthermore, because it has been reported that hypoxia is important to enhance cardiac differentiation [10], the system was capable of strict regulation of a low dissolved oxygen concentration. Collectively, the integration of mainly homogeneously sized EBs by modest agitation, a hypoxic condition and appropriate treatments with growth factors and a small molecule enabled us to successfully induce the differentiation of cardiomyocytes with high efficacy.

On the other hand, we also used a monolayer-based method for cardiac differentiation. Matrigel was overlaid on cells at 1 day prior to differentiation, and bFGF was added from day 1–4, resulting in robust cardiac differentiation at day 12. However, these cardiomyocytes showed colony-like formation after re-seeding onto the UpCell (Fig. 3F), which might lead to an unequal cardiomyocyte distribution in cell sheets. These differences in the phenotypes of cardiomyocytes between bioreactor-based and monolayer-based methods might be explained by the difference in cardiomyocyte maturation levels and the phenotype of mural cells. The optimized timing of cardiomyocyte harvesting after differentiation might overcome this limitation.

In this study, the cardiac cell sheets were mainly composed of cardiomyocytes and partially composed of mural cells. The ratio of cardiomyocytes to mural cells in a cell sheet was approximately 8:2. We previously reported that purified cardiomyocytes do not form cell sheets, and a certain level of fibroblasts is necessary to create mouse ESC-derived cardiac cell sheets with an optimized ratio of cardiomyocytes/fibroblasts of 8:2 [9].The existence of non-cardiomyocytes potentially expressing extracellular matrix components might be important to form human cardiac cell sheets. Recently, several methods have been reported for the purification of cardiomyocytes from human pluripotent stem cells using an antibody [13,17], mitochondrial labeling [18] and genetic modification [19]. These cardiomyocyte purification methods will enable us to optimize the ratio of cardiomyocytes/non-cardiomyocytes for creating more functional cardiac tissue.

Competing interests statement: Tatsuya Shimizu and Masayuki Yamato are consultants for CellSeed, Inc., Teruo Okano is an investor in CellSeed, Inc.

Acknowledgments

Appendix A. Supplementary data

Supplementary data associated with this article can be found, in the online version, at http://dx.doi.org/10.1016/j.bbrc.2012.07.089.

References

[1] T. Okano, N. Yamada, H. Sakai, Y. Sakurai, A novel recovery system for cultured cells using plasma-treated polystyrene dishes grafted with poly(N-isopropylacrylamide), J. Biomed. Mater. Res. 27 (1993) 1243–1251.

[2] A. Kushida, M. Yamato, C. Konno, A. Kikuchi, Y. Sakurai, T. Okano, Decrease in culture temperature releases monolayer endothelial cell sheets together with deposited fibronectin matrix from temperature-responsive culture surfaces, J. Biomed. Mater. Res. 45 (1999) 355–362.

[3] K. Matsuura, A. Honda, T. Nagai, N. Fukushima, K. Iwanaga, M. Tokunaga, T. Shimizu, T. Okano, H. Kasanuki, N. Hagiwara, I. Komuro, Transplantation of cardiac progenitor cells ameliorates cardiac dysfunction after myocardial infarction in mice, J. Clin. Invest. 119 (2009) 2204–2217.

[4] I.A. Memon, Y. Sawa, N. Fukushima, G. Matsumiya, S. Miyagawa, S. Taketani, S.K. Sakakida, H. Kondoh, A.N. Aleshin, T. Shimizu, T. Okano, H. Matsuda, Repair of impaired myocardium by means of implantation of engineered autologous myoblast sheets, J. Thorac. Cardiovasc. Surg. 130 (2005) 1333–1341.

[5] H. Sekine, T. Shimizu, K. Hobo, S. Sekiya, J. Yang, M. Yamato, H. Kurosawa, E. Kobayashi, T. Okano, Endothelial cell coculture within tissue-engineered cardiomyocyte sheets enhances neovascularization and improves cardiac function of ischemic hearts, Circulation 118 (2008) S145–152.

[6] H. Masumoto, T. Matsuo, K. Yamamizu, H. Uosaki, G. Narazaki, S. Katayama, A. Marui, T. Shimizu, T. Ikeda, T. Okano, R. Sakata, J.K. Yamashita, Pluripotent stem cell-engineered cell sheets reassembled with defined cardiovascular populations ameliorate reduction in infarct heart function through cardiomyocyte-mediated neovascularization, Stem Cells 30 (2012) 1196–1205.

[7] G. Olivetti, M. Melissari, J.M. Capasso, P. Anversa, Cardiomyopathy of the aging human heart. Myocyte loss and reactive cellular hypertrophy, Circ. Res. 68 (1991) 1560–1568.

[8] T. Shimizu, H. Sekine, J. Yang, Y. Isoi, M. Yamato, A. Kikuchi, E. Kobayashi, T. Okano, Polysurgery of cell sheet grafts overcomes diffusion limits to produce thick, vascularized myocardial tissues, FASEB J. 20 (2006) 708–710.

[9] K. Matsuura, S. Masuda, Y. Haraguchi, N. Yasuda, T. Shimizu, N. Hagiwara, P.W. Zandstra, T. Okano, Creation of mouse embryonic stem cell-derived cardiac cell sheets, Biomaterials 32 (2011) 7355–7362.

[10] L. Yang, M.H. Soonpaa, E.D. Adler, T.K. Roepke, S.J. Kattman, M. Kennedy, E. Henckaerts, K. Bonham, G.W. Abbott, R.M. Linden, L.J. Field, G.M. Keller, Human cardiovascular progenitor cells develop from a KDR+ embryonic-stem-cell-derived population, Nature 453 (2008) 524–528.

[11] E. Willems, S. Spiering, H. Davidovics, M. Lanier, Z. Xia, M. Dawson, J. Cashman, M. Mercola, Small-molecule inhibitors of the Wnt pathway potently promote cardiomyocytes from human embryonic stem cell-derived mesoderm, Circ. Res. 109 (2011) 360–364.

[12] M.A. Laflamme, K.Y. Chen, A.V. Naumova, V. Muskheli, J.A. Fugate, S.K. Dupras, H. Reinecke, C. Xu, M. Hassanipour, S. Police, C. O'Sullivan, L. Collins, Y. Chen, E. Minami, E.A. Gill, S. Ueno, C. Yuan, J. Gold, C.E. Murry, Cardiomyocytes derived from human embryonic stem cells in pro-survival factors enhance function of infarcted rat hearts, Nat. Biotechnol. 25 (2007) 1015–1024.

[13] H. Uosaki, H. Fukushima, A. Takeuchi, S. Matsuoka, N. Nakatsuji, S. Yamanaka, J.K. Yamashita, Efficient and scalable purification of cardiomyocytes from human embryonic and induced pluripotent stem cells by VCAM1 surface expression, PLoS One 6 (2011) e23657.

[14] P.W. Burridge, S. Thompson, M.A. Millrod, S. Weinberg, X. Yuan, A. Peters, V. Mahairaki, V.E. Koliatsos, L. Tung, E.T. Zambidis, A universal system for highly efficient cardiac differentiation of human induced pluripotent stem cells that eliminates interline variability, PLoS One 6 (2011) e18293.

[15] Q. Zhang, J. Jiang, P. Han, Q. Yuan, J. Zhang, X. Zhang, Y. Xu, H. Cao, Q. Meng, L. Chen, T. Tian, X. Wang, P. Li, J. Hescheler, G. Ji, Y. Ma, Direct differentiation of atrial and ventricular myocytes from human embryonic stem cells by alternating retinoid signals, Cell. Res. 21 (2011) 579–587.

[16] P.W. Burridge, G. Keller, J.D. Gold, J.C. Wu, Production of de novo cardiomyocytes: human pluripotent stem cell differentiation and direct reprogramming, Cell Stem Cell 10 (2012) 16–28.

[17] N.C. Dubois, A.M. Craft, P. Sharma, D.A. Elliott, E.G. Stanley, A.G. Elefanty, A. Gramolini, G. Keller, SIRPA is a specific cell-surface marker for isolating cardiomyocytes derived from human pluripotent stem cells, Nat. Biotechnol. 29 (2011) 1011–1018.

[18] F. Hattori, H. Chen, H. Yamashita, S. Tohyama, Y.S. Satoh, S. Yuasa, W. Li, H. Yamakawa, T. Tanaka, T. Onitsuka, K. Shimoji, Y. Ohno, T. Egashira, R. Kaneda, M. Murata, K. Hidaka, T. Morisaki, E. Sasaki, T. Suzuki, M. Sano, S. Makino, S. Oikawa, K. Fukuda, Nongenetic method for purifying stem cell-derived cardiomyocytes, Nat. Methods 7 (2010) 61–66.

[19] H. Kita-Matsuo, M. Barcova, N. Prigozhina, N. Salomonis, K. Wei, J.G. Jacot, B. Nelson, S. Spiering, R. Haverslag, C. Kim, M. Talantova, R. Bajpai, D. Calzolari, A. Terskikh, A.D. McCulloch, J.H. Price, B.R. Conklin, H.S. Chen, M. Mercola, Lentiviral vectors and protocols for creation of stable hESC lines for fluorescent tracking and drug resistance selection of cardiomyocytes, PLoS One 4 (2009) e5046.

ORIGINAL ARTICLE

Long-term results of a cardiovascular implantable electronic device wrapped with an expanded polytetrafluoroethylene sheet

Bun Yashiro · Morio Shoda · Yasuko Tomizawa ·
Tetsuyuki Manaka · Nobuhisa Hagiwara

Abstract The use of an expanded polytetrafluoroethylene (ePTFE) sheet wrapping device for patients with pacemaker contact dermatitis is still controversial. This study aimed to retrospectively investigate the occurrence rate of allergies and other complications after implantation of a cardiovascular implantable electronic device (CIED) wrapped with an ePTFE sheet. A total of 4,497 procedures of CIED implantation were performed at our institution between January 1993 and April 2010. Among 19 patients who underwent implantation of an electronic cardiac device wrapped with an ePTFE sheet, device implantation was performed in 11 patients for secondary prevention of device contact sensitivity, in 7 patients for primary prevention of device contact sensitivity, and in 1 patient for avoiding over-sensing of myopotentials. During follow-up periods (mean 46 ± 34 months), there were no allergic or inflammatory reactions to components of the device or ePTFE itself. Among 11 patients with a device wrapped with an ePTFE sheet for secondary prevention, 5 patients completed device replacement due to battery depletion and 3 patients had infections from the

device. Wrapping implantable devices with an ePTFE sheet is an effective way of preventing device sensitivity in patients who require CIED therapy. However, the risk of infection from the device should be taken into consideration.

Introduction

Recently, the efficacy of cardiovascular implantable electronic devices (CIEDs) for arrhythmia and heart failure, including pacemakers, implantable cardioverter-defibrillators, and cardiac-resynchronization therapy with or without an implantable defibrillator, has been demonstrated in many trials [1–3]. There has been an increase in the number of patients treated with CIEDs based on this clinical evidence, but the prevention and management of various device-related complications, such as bleeding into the generator pocket, perforation with pericardial effusion and/or tamponade, pneumothorax, and infections, are important issues [4, 5].

Contact sensitivity to components of devices is a rare complication. However, repetitive recurrence of allergies often makes it difficult to provide sufficient treatment to patients who require device therapy. Although there are case reports for the use of an expanded polytetrafluoroethylene (ePTFE) sheet wrapping device in patients with pacemaker contact dermatitis [6–11], there are few published data on the long-term efficacy of this method. Therefore, we retrospectively investigated the occurrence rate of allergies and other complications after implantation of a CIED wrapped with an ePTFE sheet.

B. Yashiro (✉) · M. Shoda · T. Manaka · N. Hagiwara
Department of Cardiology, Tokyo Women's Medical University,
8-1 Kawada-cho, Shinjuku-ku, Tokyo 162-8666, Japan
e-mail: bunyashiro@gmail.com

Y. Tomizawa (✉)
Department of Cardiovascular Surgery, Tokyo Women's
Medical University, 8-1 Kawada-cho, Shinjuku-ku,
Tokyo 162-8666, Japan
e-mail: stomizaw@hij.twmu.ac.jp

Patients and methods

Patients

A total of 4,497 procedures of CIED implantation, including new device implantation, device revision, replacement, and device upgrade, were performed at our institution between January 1993 and April 2010. Nineteen patients underwent implantation of an electronic cardiac device wrapped with an ePTFE sheet. Eleven out of 19 patients had device revision with the use of an ePTFE sheet for secondary prevention of device contact sensitivity occurring after the previous implantation (Figs. 1 and 2). The other 8 patients did not have previous skin symptoms and 7 of them were previously diagnosed with a metallic allergy. The remaining 1 patient was diagnosed with over-sensing of myopotentials. The incidence of device contact sensitivity was 2.4 per 1,000 procedures.

Skin reactions on the generator pocket site, such as redness, swelling, erosion, fistulation and others, were observed in the outpatient clinic after initial implantation in 5 of them, and after re-implantation in 6. The time to symptoms widely varied, ranging from 2 weeks to 72 months (mean time 26 ± 26 months) after implantation. In 7 patients with a past history of a metal allergy, an ePTFE sheet was used for primary prevention at the initial device implantation. In only 1 patient, an ePTFE sheet was used for prevention of over-sensing of myopotentials, which had been recognized in a scheduled pacemaker clinic.

The mean follow-up duration after device implantation with an ePTFE sheet was 46 ± 34 months, the mean age at ePTFE use was 60 ± 14 years, and 9 patients were male (Table 1).

Diagnosis

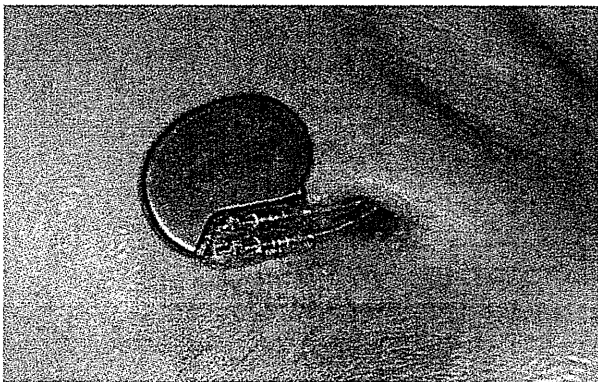Diagnosis of contact sensitivity to device-related materials in patients with CIED was made when patients had localized skin reactions on the generator-pocket site, a negative blood culture, a negative tissue culture from the generator-pocket site, and no other suggestive features for infections, considering results of skin patch tests and a past history of contact dermatitis to metals.

In skin patch tests, specimens from all the pacemaker and lead components obtained from the device manufacturers and generator itself were directly applied to the patient's skin and removed after 48 h (Fig. 3). According to the North American Contact Dermatitis Group criteria, patch test reactions were evaluated initially on the day of removal of the allergens from the skin, and then again 2–3 days later [12]. A total of 12 patients had the skin


Fig. 2 The wrapping of a new generator and leads with an ePTFE sheet during the procedure of device revision in a patient with device sensitivity

Table 1 Clinical characteristics of patients with a device wrapped with an ePTFE sheet

Characteristics	Patients
n	19
Age (years)	60
Male, n (%)	9 (47)
Mean follow-up duration (months)	46 ± 34
Arrhythmia	
AV block, n (%)	9 (47)
Sick sinus syndrome, n (%)	4 (21)
Atrial fibrillation, n (%)	5 (26)
Ventricular tachycardia, n (%)	2 (11)
Brugada syndrome, n (%)	2 (11)
Heart failure, n (%)	3 (16)
Device	
Pacemaker, n (%)	14 (74)
ICD, n (%)	2 (11)
CRTP/CRTD, n (%)	3 (15)

AV atrioventricular, ICD implantable cardioverter-defibrillator, CRTP cardiac-resynchronization therapy with a pacemaker, CRTD cardiac-resynchronization therapy with a pacemaker-defibrillator

Fig. 1 Exposure of a pacemaker in a patient with pacemaker sensitivity

Fig. 3 Skin patch tests of specimens from all the pacemaker and lead components obtained from the device manufacturers (a) and generator (b)
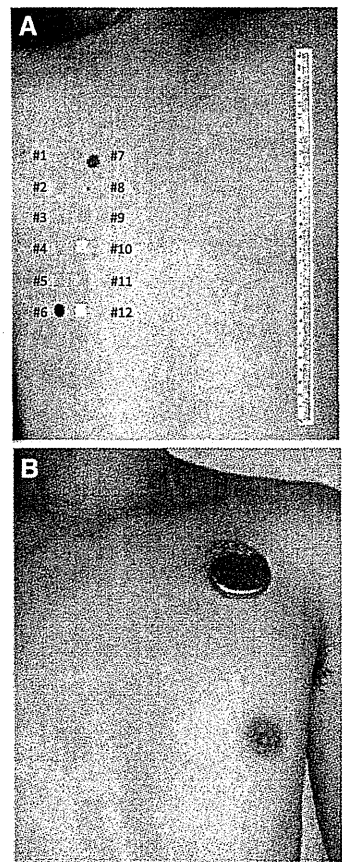
Allergy test samples provided from Medtronic Japan.
#1 Polyurethane (80A)
#2 Polyurethane (75D)
#3 Silicon rubber (MDX-70)
#4 Silicon rubber (ETR-50)
#5 Silicon-medical adhesive
#6 Titanium
#7 Parylene coated titanium
#8 Platinum iridium
#9 Polysulfone (AMBER)
#10 Polysulfone (BEIGE)
#11 Silicon rubber (MED 4719)
#12 Barium sulfate filled silicon rubber

patch test for either device-related materials or a generator, or both, 9 patients had a device-related materials patch test and 11 patients had a generator patch test. The other 7 patients were previously diagnosed with a metallic allergy and patch tests were not performed to avoid the risk of induction of device contact sensitivity.

Operative use of an ePTFE sheet

CIED implantation was performed by skillful cardiologists in a catheter laboratory. Both the generator and lead were placed together and wrapped with an ePTFE sheet (Gore-Tex Surgical Membrane; W.L. Gore & Associates, Flag-staff, AZ, USA), and then the wrapped device system was implanted at the pocket in layers of deep fascia of the pectoralis major. Administration of antimicrobial therapy was started at implantation and continued for 3 days.

Results

Skin patch tests at diagnosis of a device allergy

Four (44%) of the 9 patients evaluated with skin patch tests of device-related material series had positive results to

Table 2 Results of skin patch tests

	Positive	Negative
Device-related materials, n (%)	4 (44)[a]	5 (56)
Generator, n (%)	6 (55)	5 (45)

[a] Positive results were found in nickel ($n = 1$), manganese ($n = 1$), zinc ($n = 1$), titanium ($n = 2$), silicone ($n = 1$), and polychloroparaxylene ($n = 1$)

titanium, nickel, manganese, zinc, polychloroparaxylene, and silicon (Table 2). Six (55%) of the 11 patients evaluated with skin patch tests of a generator patch test had positive results. Skin patch tests were not performed in 7 patients who were considered to have a risk of sensitization to materials.

Outcomes

There was no allergic or inflammatory reaction to components of the device and ePTFE itself. Among 11 patients with a device wrapped with an ePTFE sheet for secondary prevention, 5 patients completed device replacement due to battery depletion and 3 had device infections (Table 3). The profile of the 3 patients with device infection is shown in Table 4. In patients 1 and 2, skin reactions concomitant

with a fistula of the generator pocket site had occurred 10 months after first implantation and 39 months after pacemaker replacement, respectively, without any signs of infection. Therefore, a pacemaker wrapped with an ePTFE sheet was implanted at the contralateral side after antimicrobial therapy. However, patients 1 and 2 had pocket infection with *Mycobacterium chelonae*, and methicillin-sensitive *Staphylococcus aureus* was identified as a pathogen by tissue culture from the pocket site, 27 months and 1 month after implantation, respectively.

Discussion

In the present study, we found that an ePTFE sheet was a reliable material for preventing an allergic reaction or inflammation to components of a CIED, but there was also a possibility of increasing the risk of infection from the device. Few reports have described the long-term efficacy or complications of a wrapping device with an ePTFE sheet, although there are several cases reported in the literature on the use of this material for avoiding allergies [6–11]. To the best of our knowledge, this is the first report describing the clinical course of patients with a CIED wrapped with an ePTFE sheet.

During the follow-up period, we did not observe an allergic reaction or inflammation to device-related materials and ePTFE itself in study patients with a CIED wrapped

with an ePTFE sheet. An ePTFE is a biocompatible material and has many other properties, including strength (high strength-to-weight ratio), high chemical resistance, low water adsorption, low flammability, and high thermal resistance. It is considered extremely rare that an ePTFE, which is widely used in the medical field, such as a vascular graft or pericardial substitute, causes inflammation after implantation. The results of the present study support the reliability of an ePTFE as a material for prevention of device sensitivity.

Implanted devices have the potential to cause an immune reaction between components of devices and the recipient. Therefore, CIEDs are made of materials that should have excellent biocompatibility, including titanium, polyurethane, silicon, and polychloroparaxylene. In spite of their excellent biocompatibility, however, there are several reports of allergies to these materials in patients with CIED [6, 13–18]. Tomizawa et al. [15] reported that titanium is corroded by contact with body fluid and that severe inflammation and immunocytes are activated by released metal ions. It is known that metal allergies develop following repeated or prolonged skin contact with metal ions [19], although the detailed mechanisms of immune reaction to metals remain unclear. Allergic reactions to metals occur in a few days or weeks after sensitization by antigen-specific T cells [19]. However, in the present study, the time to skin reaction varied from a few weeks to years after initial implantation or replacement, which is similar to published data [3, 4, 6, 18, 20, 21]. This suggests that immunological foreign body reactions to components of devices are induced with various timings under each condition of the recipient and device.

Another important finding of our study is that the rate of infection from the device in patients with devices wrapped with an ePTFE sheet was higher than that in the general CIED population [22]. It occurred at a high rate of 16% in patients with devices wrapped with an ePTFE sheet for secondary prevention to device sensitivity in the current study. There may be several explanations for susceptibility to infection in these patients. First, additional maneuvers of wrapping devices with an ePTFE sheet and/or an increased

Table 3 Outcomes in patients with a device wrapped with an ePTFE sheet

	Patients			Total (n = 19)
	Primary (n = 7)	Secondary (n = 11)	Over-sensing (n = 1)	
No. events	7	3	1	11
Replacement	0	5	0	5
Device infection	0	3	0	3

Table 4 Profiles of 3 patients with device infection after use of an ePTFE sheet

Patient	Device	Skin reactions	Time to skin reactions (months)	Patch tests of device-related materials/generator	ePTFE implantation site	Time to infection (months)	Cultured bacteria
1	PM	Redness, swelling, fistula	10	Neg/pos	Contralateral	27	*Mycobacterium chelonae*
2	PM	Redness, swelling, fistula, blister	39	Neg/neg	Contralateral	1	MSSA
3	ICD	Redness, thinning	20	Neg/neg	Same	2	*S. epidermidis*

PM pacemaker, *ICD* implantable cardioverter-defibrillator, *neg* negative result, *pos* positive result, *MSSA* methicillin-sensitive *Staphylococcus aureus*

amount of indwelling hardware may increase the risk of infection as a periprocedural factor, which is indicated as one of the risk factors of CIED infection in a current guideline [22]. Moreover, pools of exudates around indwelling hardware or an irregular surface of the device wrapped with an ePTFE sheet may favor microbial adherence [22]. Two of 3 patients with device infection in our study were infected within 2 months after implantation, suggesting participation of these periprocedural factors. Second, it is generally difficult to make a definitive diagnosis of device allergies because of a low sensitivity and specificity of skin patch tests [13, 20]. Some patients with infection from a device have negative tissue culture results from the pocket site and no other signs of infection apart from swelling or redness of skin at the pocket site [7, 23], which make it difficult to differentiate infection from an allergy due to the device. These findings suggest that clinical signs of device contact sensitivity and infection can overlap with each other, and therefore, careful differential diagnosis of allergies and infections from devices is needed. Even if an allergy from the device is strongly suspected as a cause of skin reactions at the generator pocket site, the existence of local pocket infection when a fistula or erosion is present, even in the absence of signs of infection, should be considered. In such cases, management of CIED infection, including CIED removal, needs to be prioritized. Wilkerson and Jordan reported pressure dermatitis following an isomorphic response to expansion of the subcutaneous tissues by a hard device, which should be distinguished from infection or contact dermatitis [24]. An implanted device can cause an isomorphic response, which may be attributable to the local mechanical or anatomic features of the individual. In such cases, dermatitis overlying the generator-pocket site can be eliminated by replacement at the new anatomic site, which is more tolerant of rubbing on compression.

Conclusion

We conclude that wrapping with an implantable device with an ePTFE sheet is an effective way of preventing device sensitivity in patients who require CIED therapy. However, there is a risk of device infection, and an attentive implantation procedure and careful differential diagnosis of allergies and infections from devices are needed.

References

1. Moss AJ, Zareba W, Hall J, Klein H, Wilber DJ, Cannom DS, Daubert JP, Higgins S, Brown M, Andrews ML, For the Multicenter Automatic Defibrillator Implantation Trial II Investigators. Prophylactic implantation of a defibrillator in patients with myocardial infarction and reduced ejection fraction. N Engl J Med. 2002;346:877–83.
2. Brady GH, Mark DB, Poole JE, Packer DL, Boineau R, Domanski M, Troutman C, Anderson J, Johnson G, McNulty SE, Clapp-Channing N, Davidson LD, Fraulo ES, Fishbein DP, Luceri RM, John H, For the Sudden Cardiac Death in Heart Failure Trail (SCD-HeFT) investigators. Amiodarone or an implantable cardioverter-defibrillator for congestive heart failure. N Engl J Med. 2005;352:225–37.
3. Bristow MR, Saxon LA, Boehmer J, Krueger S, Kass DA, Marco TD, Carson P, DiCarlo L, DeMets D, White BG, DeVries DW, Feldman AM, For the Comparison of Medical Therapy, Pacing, and Defibrillation in Heart Failure (COMPANION) Investigators. Cardiac-resynchronization therapy with or without an implantable defibrillator in advanced chronic heart failure. N Engl J Med. 2004;305:2140–50.
4. Stevenson WG, Chaitman BR, Ellenbogen KA, Epstein AE, Gross WL, Hayes DL, Strickberger SA, Sweeney MO, For the Subcommittee in Electrocardiography and Arrhythmias of the American Heart Association Council on Clinical Cardiology, in Collaboration With the Heart Rhythm Society. Clinical assessment and management of patients with implanted cardioverter-defibrillators presenting to nonelectrophysiologists. Circulation. 2004;110:3866–9.
5. Sawa Y, Tatsumi E, Funakubo A, Horiuchi T, Iwasaki K, Kishida A, Masuzawa T, Matsuda K, Myoui A, Nishimura M, Nishimura T, Tokunaga S, Tomizawa Y, Tomo T, Tsukiya T, Yamaoka T. Journal of artificial organs 2010: the year in review. J Artif Organs. 2011;14:1–8.
6. Iguchi N, Kasanuki H, Matsuda N, Shoda M, Ohnishi S, Hosoda S. Contact sensitivity to polychloroparaxylene-coated cardiac pacemaker. PACE. 1997;20:372–3.
7. Ishii K, Kodani E, Miyamoto S, Otsuka T, Hosone M, Ogata K, Sato W, Matsumoto S, Tadera T, Ibuki C, Kusama Y, Atarashi H. Pacemaker contact dermatitis: the effective use of a polytetrafluoroethylene sheet. PACE. 2006;29:1299–302.
8. Yamamoto M, Uchiyama M, Nakajima S, Hanyaku H, Suda Y, Niinami H, Kono K, Tabata M, Sasaki A, Asano R, Ikeda M, Kataoka G, Harada T, Takeuchi Y. Two cases of pacemaker allergic dermatitis treated with polytetrafluoroethylene sheet. Ther Res. 2004;25:991–8. (in Japanese).
9. Kono K, HaraK, Higashi T, Watanabe S, Asakawa H, Ono H, Horinaka S, Matsuoka H, Mochizuki Y, Yamada Y, Mori H, Okamura Y. Pacemaker contact dermatitis treated with polytetrafluoroethylene sheet. J Arrhythmia 2000;16:403–7 (in Japanese).
10. Fujimori M, Akagi T, Tanabe M, Matsumoto N. Patients with metal allergy after implantation of a pacemaker. J Arrhythmia. 2003;19:79–83. (in Japanese).
11. Tamenishi A, Usui A, Oshima H, Ueda Y. Entirely polytetrafluoroethylene coating for pacemaker system contact dermatitis. Interact Cardiovasc Thorac Surg. 2008;7:275–6.
12. Marks JG Jr, Belsito DV, DeLeo VA, Fowler JF Jr, Fransway AF, Maibach HI, Mathias CG, Pratt MD, Rietschel RL, Sherertz EF, Storrs FJ, Taylor JS. North American Contact Dermatitis Group patch-test results, 1998 to 2000. Am J Contact Dermat. 2003;14:59–62.
13. Peters MS, Schroeter AL, van Hale HM, Broadbent JC. Pacemaker contact sensitivity. Contact Dermat. 1984;11:214–8.
14. Viraben R, Boulinguez S, Alba C. Granulomatous dermatitis after implantation of a titanium containing pacemaker. Contact Dermat. 1995;33:437.
15. Tomizawa Y, Hanawa T. Corrosion of pure titanium sternal wire. Ann Thorac Surg. 2007;84:1012–4.

16. Dery JP, Gilbert M, O'Hara G, Champagne J, Desaulniers D, Cartier P, Philippon F. Pacemaker contact sensitivity: case report and review of the literature. PACE. 2002;25:863–5.

17. Oprea ML, Schnoring H, Sachweh JS, Ott H, Biertz J, Vazquez-Jimenez JF. Allergy to pacemaker silicone compounds: recognition and surgical management. Ann Thorac Surg. 2009;87:1275–7.

18. Raque C, Goldschmidt H. Dermatitis associated with an implanted cardiac pacemaker. Arch Dermatol. 1970;102:646–9.

19. Thyssen JP, Menne T. Metal allergy: a review on exposures, penetration, genetics, prevalence, and clinical implication. Chem Res Toxicol. 2010;23:309–18.

20. Yamauchi R, Morita A, Tsuji T. Pacemaker dermatitis from titanium. Contact Dermat. 2000;42:52–3.

21. Brun R, Hunziker N. Pacemaker dermatitis. Contact Dermat. 1980;6:212–3.

22. Baddour LM, Epstein AE, Erickson CC, Knight BP, Levison ME, Lackhart PB, Masoudi FA, Okum EJ, Wilson WR, Beerman LB, Bolger AF, Estes NAM 3rd, Gewitz M, Newburger JW, Schron EB, Taubert KA; on behalf of the American Heart Association Rheumatic Fever, Endocarditis, and Kawasaki Disease Committee of the Council on Cardiovascular Disease in the Young; Council on Cardiovascular Surgery and Anesthesia; Council on Cardiovascular Nursing; Council on Clinical on Cardiology; and the Interdisciplinary Council on Quality of Care and Outcomes Research. Update on cardiovascular implantable electronic device infections and their management: a scientific statement from the American Heart Association. Circulation. 2010;121:458–77.

23. Dy Chua J, Abdul-Karim A, Mawhorter S, Procop GW, Tchou P, Niebauer M, Saliba W, et al. The role of swab and tissue culture in the diagnosis of implantable cardiac device infection. Pacing Clin Electrophysiol 2005;28:1276–81.

24. Wilkerson MG, Jordan WP. Pressure dermatitis from an implanted pacemaker. Dermatol Clin. 1990;8:189–92.

Estradiol triggers sonic-hedgehog-induced angiogenesis during peripheral nerve regeneration by downregulating hedgehog-interacting protein

Haruki Sekiguchi[1,2], Masaaki Ii[1,3], Kentaro Jujo[1,2], Marie-Ange Renault[1,4,5], Tina Thorne[1], Trevor Clarke[1], Aiko Ito[1], Toshikazu Tanaka[1,6], Ekaterina Klyachko[1], Yasuhiko Tabata[7], Nobuhisa Hagiwara[2] and Douglas Losordo[1]

Both estradiol (E2) and Sonic Hedgehog (Shh) contribute to angiogenesis and nerve regeneration. Here, we investigated whether E2 improves the recovery of injured nerves by downregulating the Shh inhibitor hedgehog-interacting protein (HIP) and increasing Shh-induced angiogenesis. Mice were treated with local injections of E2 or placebo one week before nerve-crush injury; 28 days after injury, nerve conduction velocity, exercise duration, and vascularity were significantly greater in E2-treated mice than in placebo-treated mice. E2 treatment was also associated with higher mRNA levels of Shh, the Shh receptor Patched-1, and the Shh transcriptional target Gli1, but with lower levels of HIP. The E2-induced enhancement of nerve vascularity was abolished by the Shh inhibitor cyclopamine, and the effect of E2 treatment on Shh, Gli1, and HIP mRNA expression was abolished by the E2 inhibitor ICI. Gli-luciferase activity in human umbilical-vein endothelial cells (HUVECs) increased more after treatment with E2 and Shh than after treatment with E2 alone, and E2 treatment reduced HIP expression in HUVECs and Schwann cells without altering Shh expression. Collectively, these findings suggest that E2 improves nerve recovery, at least in part, by reducing HIP expression, which subsequently leads to an increase in Shh signaling and Shh-induced angiogenesis.

The physiological effects of estrogen extend well beyond its role in development and menstrual-cycle regulation. Estrogen exists in multiple forms: estrone sulfate, which is inactive and has a relatively long half-life in peripheral blood; estrone, the active product of estrone sulfate metabolism; and estradiol (E2), the active product of estrone metabolism by 17β-hydroxysteroid dehydrogenase type 1. Because serum E2 levels are inversely correlated with the onset of cardiovascular disease in postmenopausal women,[1] E2 was investigated for the prevention of cardiovascular disease in several clinical trials of hormone replacement therapy.[2,3]

Evidence indicates that E2 reduces the risk of cardiovascular events in younger postmenopausal women.[4,5] The favorable effects of E2 may be partly attributed to enhanced angiogenesis: functional estrogen receptors are essential for the induction of angiogenesis by basic fibroblast growth factor,[6] and estrogen accelerates endothelial recovery by increasing nitric oxide production and enhancing the mobilization of bone marrow-derived endothelial progenitor cells.[7] E2 also appears to contribute to the preservation and recovery of injured nerve tissue: the expression of estrogen receptors α and β increases after nerve injury,[8] and implantation of E2-containing pellets one week before nerve-crush injury stimulated nerve preservation/regeneration,[9] perhaps by activating mitogen-activated protein kinase signaling.[8] E2 also protects against ischemia-induced neural death by activating the Akt pathway.[10]

[1]Feinberg Cardiovascular Research Institute and Program in Cardiovascular Regenerative Medicine, Division of Cardiovascular Medicine, Department of Medicine, Northwestern University Feinberg School of Medicine and Northwestern Memorial Hospital, Chicago, IL, USA; [2]Department of Cardiology, Tokyo Women's Medical University, Tokyo, Japan; [3]Group of Translational Stem Cell Research, Department of Pharmacology, Osaka Medical College, Osaka, Japan; [4]Université de Bordeaux, Adaptation cardiovasculaire à l'ischémie, Pessac, France; [5]INSERM, U1034, Adaptation cardiovasculaire à l'ischémie, Pessac, France; [6]University of Pittsburgh Medical Center, Pittsburgh, PA, USA and [7]Department of Biomaterials, Field of Tissue Engineering, Institute for Frontier Medical Sciences, Kyoto University, Kyoto, Japan
Correspondence: Dr M Ii, MD, PhD, Group of Translational Stem Cell Research, Department of Pharmacology, Osaka Medical College, 2-7, Daigaku-machi, Takatsuki, Osaka 569-8686, Japan.
E-mail: masa0331@mac.com